Tutor

Dr. Joaquín F. Pérez de Benito
Departament de Ciència de Materials i Química Física

Grau de Química

Treball Final de Grau

Kinetic study of the complexation of chromium(III) by L-glutamic acid

Estudi cinètic de la complexació de crom(III) per l'àcid L-glutàmic

Joan Nicolàs Rivasés

June 2017

Universitat de Barcelona

B:KC Barcelona Knowledge Campus
Campus d'Excel·lència Internacional

It is the tension between creativity and skepticism that has produced the stunning and unexpected findings of science.

Carl Sagan

In the first place, I would like to express my gratitude to Dr. Joaquín Fernando Pérez de Benito. His experience in this research field has made possible for me to grasp more easily the fundamentals of chemistry required to understand the present study.

I am also indebted to my parents and girlfriend for their patience, motivation and continuous support. Without them, this work would have not been the same.

REPORT

CONTENTS

1. SUMMARY

The complexation of chromium(III) by L-glutamic acid / hydrogen L-glutamate ion in aqueous media under slightly acidic conditions (pH 2.46 – 5.87) has been studied by the use of UV-Vis spectroscopy. Although the reaction in the presence of a large excess of organic ligand is considered in the chemical literature to be a pseudo-first order kinetic process, the rate-time plots corresponding to the formation of the reaction product show a distinct bell-shaped profile, caused by the accumulation of a long-lived intermediate. Given that this intermediate is not reactive enough for the steady state approximation to apply, an integrated rate law involving a double-exponential function has been used to obtain two rate constants for each kinetic experiment, corresponding to the formation of the long-lived intermediate from the reactants (k_1) and to its decay into the reaction products (k_2). Both rate constants increased with the initial concentration of hydrogen L-glutamate ion in a double-reciprocal linear relationship, k_1 decreased with the ionic strength whereas k_2 increased, both evidenced the existence of base catalysis and the corresponding activation energies were 83 ± 10 and 95 ± 5 kJ mol^{-1}, respectively. The spectroscopic data indicated the formation of several complexes, differing in the number of organic ligands per chromium atom and in their acid-base properties. A mechanism in agreement with the available experimental data has been proposed, involving the breakage of a Cr(III)-aqua chemical bond as a previous step to the coordination of the organic ligand.

Keywords: chromium(III), complexation reaction, kinetics, L-glutamic acid, long-lived intermediate.

2. RESUM

S'ha estudiat la reacció de complexació del crom(III) per àcid L-glutàmic / ió hidrogen L-glutamat, en medi aquós sota condicions lleugerament àcides (pH 2.46 – 5.87) mitjançant la tècnica espectroscòpica UV-Vis. Malgrat que aquesta reacció, en presència de gran excés de lligand orgànic, és considerada a la literatura química com un procés cinètic de pseudo-primer ordre, els gràfics velocitat-temps obtinguts experimentalment corresponents a la formació del producte mostren un perfil distintiu en forma acampanada, causat per l'acumulació d'una espècie química intermèdia de llarga vida. Donat que aquest intermedi de reacció no és suficientment reactiu com per a que es pugui aplicar l'aproximació de l'estat estacionari, s'ha utilitzat una llei integrada de velocitat, la qual consisteix en una doble funció exponencial que ha permès obtenir dues constants de velocitat per a cada experiment, corresponents a la formació d'intermedi a partir dels reactius de partida (k_1) i a la seva conversió en els productes de reacció (k_2). Ambdues constants de velocitat augmenten amb la concentració inicial d'ió hidrogen L-glutamat en una relació lineal doblement recíproca, k_1 decreix amb la força iònica mentre que k_2 augmenta, totes dues evidencien l'existència de catàlisi bàsica i les seves corresponents energies d'activació són 83 ± 10 i 95 ± 5 kJ mol^{-1}, respectivament. Les dades espectroscòpiques indiquen que té lloc la formació de diversos complexos, els quals difereixen en el nombre de lligands orgànics per àtom de crom i en les seves propietats àcid-base. S'ha proposat un mecanisme de reacció coherent amb les dades experimentals disponibles, involucrant la ruptura d'un enllaç químic Cr(III)-aqua com a etapa prèvia a la coordinació amb el lligand orgànic.

Paraules clau: àcid L-glutàmic, cinètica, crom(III), intermedi de llarga vida, reacció de complexació.

3. INTRODUCTION

Chromium(III) complexes are of notable importance from the points of view of both chemistry and biology. In the first case, they constitute the final reduction products of many Cr(VI) reactions.[1-3] In the second case, chromium in its +III oxidation state is considered an oligo element involved in carbohydrate metabolism[4,5] because of its participation in the formation of the so-called glucose tolerance factor (GTF).[6-8] Although the structure of this biomolecule remains still unknown, complexation of Cr(III) by nicotinic acid and the tripeptide glutathione (cysteine-glutamic acid-glycine) is suspected. Hence, Cr(III) supplementation might play a role in the prevention and control of type 2 diabetes.[9,10] Another biomolecule involved in carbohydrate metabolism is the oligopeptide chromodulin, a part of the self-enhancing system of the insulin signal, that contains four anion-bridged Cr(III) atoms along with the amino acids asparagine, glutamine, glycine and cysteine.[11] Moreover, Cr(III) might have a role in life extension, since it leads to notable increases in both median and maximum lifespan in rodents.[12] However, large doses of supplemented Cr(III) might have some unforeseen toxic side effects.[13]

On the other hand, L-glutamic acid is one of the 21 different amino acids that constitute the building blocks of proteins. It is classified as a non-essential amino acid because it can be synthesized by the human body.[14] Its participation in the tripeptide glutathione makes this amino acid indispensable as a detoxifier and as a part of the antioxidant machinery of the cell.[15,16] In the latter case, the enzymes of the type glutathione peroxidase catalyze the reduction of both hydrogen peroxide and lipid hydroperoxides by the thiol group of glutathione.[17] Moreover, in the form of sodium hydrogen glutamate, it can be used as a food additive for the purpose of enhancing taste.[18]

All the complexes of Cr(III) are octahedral, with the metal ion (d^2sp^3 electron configuration) in the center and the six ligands occupying the vertices. The most notable feature of these complexes is their substitution inertness.[19-21] It is precisely because of this peculiarity that the reactions of replacement of the water ligands in hexaaquachromium(III) ion are slow enough to be followed by conventional spectrophotometry. In particular, kinetic studies on the complexation of Cr(III) by the amino acids DL-leucine,[22] DL-lysine[23] and L-glutamic acid[23] have been published. Although they have been reported to be of pseudo-first order under conditions of ligand/metal ion large excess, the experimental results indicate the existence of a clear-cut

deviation from this simple kinetic behavior. This anomaly seems to be ubiquitous in the reactions of Cr(III) with ligands containing both carboxyl and amino groups, the high electron density oxygen and nitrogen atoms being the active sites for the coordination with the metal ion. This is the case of the complexation of Cr(III) by picolinic acid,[24] EDTA (of notable importance in undergraduate laboratory chemistry as a teaching experiment in chemical kinetics) [25-28] and other analogous chelating agents.[29] In the present study, the stoichiometric and kinetic aspects of the reaction of Cr(III) with L-glutamic acid to form a violet complex will be addressed, and the experimental data obtained will be fitted using a two rate constant kinetic model.

4. OBJECTIVES

The aim of this investigation is to carry out a kinetic study of the ligand exchange of aqua-chromium(III) complexes by L-glutamic acid / hydrogen L-glutamate ion in moderately acidic aqueous solutions. Although the chemical literature describes this reaction as a pseudo-first-order process (under conditions of a large ligand/metal excess), the experiments show an autocatalytic-like behavior, evidenced by the observation of bell-shaped rate-time plots. However, the reaction is not actually autocatalytic, the reason for its unusual kinetics being the involvement of a long-lived intermediate in the mechanism, whose low reactivity precludes the application of the steady state approximation. The present work will focus on the nature of the long-lived intermediate, as well as on the elementary chemical steps leading to its formation from the reactants and to its conversion into the final products. To attend that objective, experimental determinations of the rate constants corresponding to both the formation and decay of the long-lived intermediate under different reactant mixture conditions will be carried out in a systematic way. Besides this kinetic information, it is expected that an analysis of the UV-Vis spectroscopy data will shed some light upon the nature and number of the final complexes formed as reaction products.

5. EXPERIMENTAL SECTION

5.1. MATERIALS AND METHODS

The solvent used in all the experiments was water previously purified by deionization followed by treatment with a Millipore Synergy UV system (milli-Q quality, κ = 0.05 μS/cm at 25.0 ºC). The reactants used in the experiments were chromium(III) nitrate nonahydrate [$Cr(NO_3)_3 \cdot 9H_2O$, Merck, purity ≥ 98.0%], L-glutamic acid [HOOC-CH(NH_2)-(CH_2)$_2$-COOH, Sigma-Aldrich, purity ≥ 99.5%], sodium hydrogen L-glutamate [HOOC-CH(NH_2)-(CH_2)$_2$-COONa, Sigma-Aldrich, purity ≥ 98.0%] and potassium hydroxide (KOH, Merck, purity ≥ 85%). The ionic strength was varied in some experiments by addition of potassium nitrate (KNO_3, Merck, purity ≥ 99.0%).

The pH measurements were performed by means of a Metrohm 605 pH-meter, provided with a digital presentation until the third decimal figure (± 0.001 pH) and a combination electrode, calibrated with the aid of commercial buffers of known pH (Sigma-Aldrich). The temperature was kept constant by means of a Julabo thermostatic bath provided with a digital reading (± 0.1 ºC). The kinetic runs were followed measuring periodically the absorbances at five different wavelengths (time intervals: 5-300 s) with a Shimadzu 160 A UV-Vis spectrophotometer (± 0.001 *A*). Simultaneously, a periodic scanning of the UV-Vis spectra (wavelength: 320-700 nm) was recorded at 1-hour time intervals with the aid of a second spectrophotometer (SI Analytics, UVLine 8100 model).

5.2. KINETIC EXPERIMENTS

In some of the runs, the initial concentration of the complexing agent, L-glutamic acid, was much higher than that of the metallic ion, Cr(III), in order to attain an approximately constant concentration of the organic reactant (isolation method). The total solution volume was kept constant in all the experiments (51 mL). In order to minimize the experimental errors associated with the kinetic data, of the five wavelengths used to monitor the reaction the one chosen to perform the calculations was that leading to a higher increment of the solution absorbance between the initial and final points. Usually, the optimal wavelength (530 – 555 nm) was slightly lower than the highest absorbance peak of the Cr(III)-glutamic acid violet complex (534 – 568 nm). With the objective to confirm the reproducibility of the kinetic determinations, all the experiments were duplicated.

5.3. CALCULATIONS AND GRAPHICS

The hardware used in the present work was a Sony Vaio personal computer, the software employed for the calculations was the programming language BBC BASIC (version for Windows) and for the graphics the program KaleidaGraph (version 4.03).

6. UV-VIS SPECTROSCOPY DATA

The electronic spectra of the inorganic reactant (blue at low pH and green at high pH) and the final violet product have been recorded (Figure 1). Although both species present two absorption peaks in the visible region of the spectrum, the absorbances at the maxima are higher for the product than for the reactant, whereas the abscissas corresponding to the former are shifted toward lower wavelengths with respect to those of the latter. These differences between the two spectra will be useful in the kinetic study to follow the progress of the reaction.

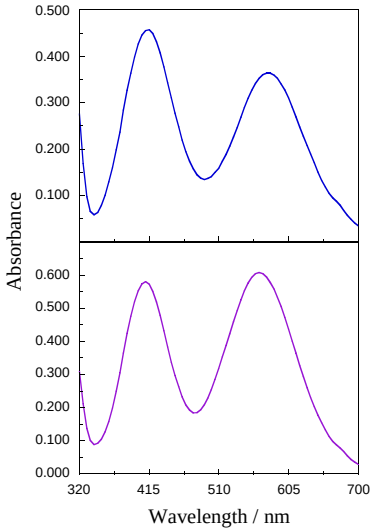

Figure 1. UV-Vis spectra of the blue metal ion (top, t = 0) and the final violet complex (bottom, t = 14 days). $[Cr(NO_3)_3]_o$ = 2.65 × 10^{-2} M, [L-glutamic acid]$_o$ = 3.92 × 10^{-2} M, $[KOH]_o$ = 1.62 × 10^{-2} M, pH 2.59, 25.0 ºC.

The UV-Vis spectrum of the reacting mixture was recorded at 1-hour time intervals (Figure 2). As the reaction advanced, the absorbance increased at most wavelengths of the visible region and, simultaneously, the two peaks suffered a certain shift toward lower wavelengths.

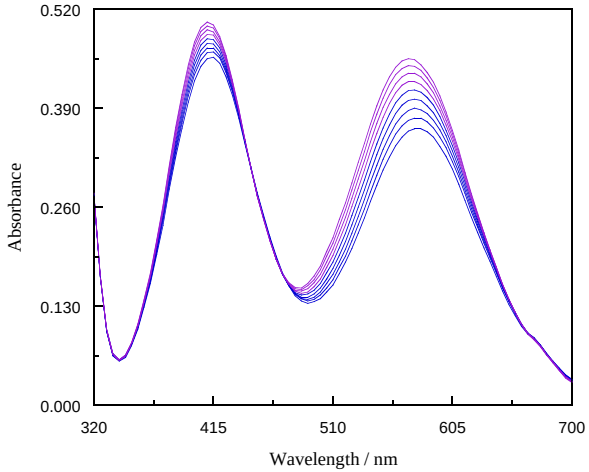

Figure 2. Periodic scanning of the UV-Vis spectrum at 1-hour time intervals during the course of the process. The shift from blue to violet indicates the progress of the reaction from reactants to products. $[Cr(NO_3)_3]_o$ = 2.65 × 10^{-2} M, [L-glutamic acid]$_o$ = 3.92 × 10^{-2} M, $[KOH]_o$ = 1.62 × 10^{-2} M, pH 2.59, 25.0 ºC.

An increase of the Cr(III) initial concentration resulted in a shift of the two absorption peaks recorded for the final violet complex toward higher wavelengths (Figure 3, bottom). As could be easily anticipated, the corresponding maximum absorbances increased indeed, but the plots were not linear, showing a downward-concave curvature instead (Figure 3, top).

On the contrary, an increase of the L-glutamic acid initial concentration resulted in a shift of the two spectral absorption peaks for the final violet complex toward lower wavelengths (Figure 4, bottom). As observed before for the metal ion, the corresponding maximum absorbances increased, but the plots were not linear, showing a downward-concave curvature instead (Figure 4, top).

The electronic spectra for the final reaction products obtained using sodium hydrogen L-glutamate as organic ligand confirmed the results previously found for L-glutamic acid (Figures 5 and 6).

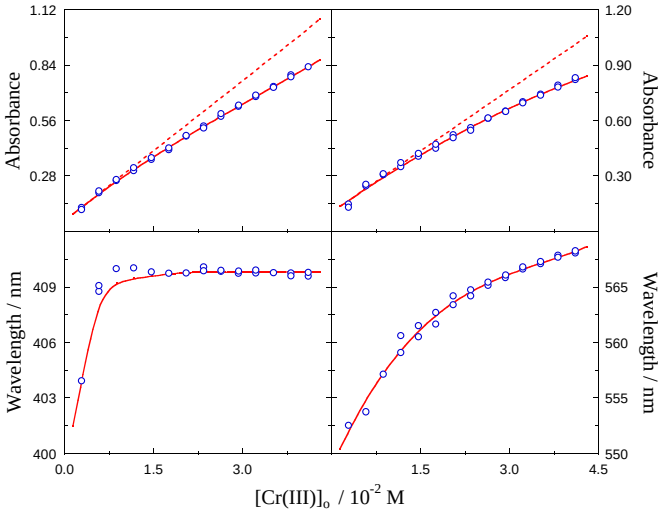

Figure 3. Wavelengths (bottom) and absorbances (top) corresponding to the first (left) and second (right) peaks of the electronic spectrum recorded for the final violet complex at different initial concentrations of metal ion. The dashed lines are the tangents to the curves at the beginning of the reaction. $[Cr(NO_3)_3]_o$ = (0.29 – 4.12) × 10^{-2} M, [L-glutamic acid]$_o$ = 3.92 × 10^{-2} M, $[KOH]_o$ = 1.62 × 10^{-2} M, pH 2.46 – 3.57, 25.0 ºC.

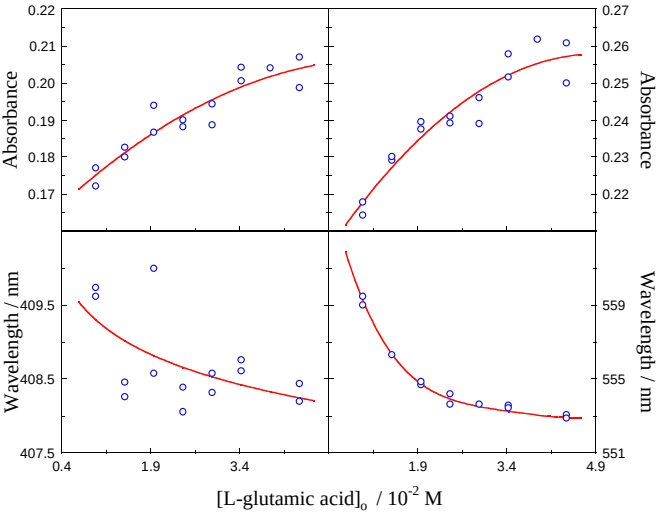

Figure 4. Wavelengths (bottom) and absorbances (top) corresponding to the first (left) and second (right) peaks of the electronic spectrum recorded for the final violet complex at different initial concentrations of organic ligand. $[Cr(NO_3)_3]_o$ = 5.88 × 10^{-3} M, [L-glutamic acid]$_o$ = (0.98 – 4.41) × 10^{-2} M, $[KOH]_o$ = 1.96 × 10^{-2} M, pH 3.37 – 3.88, 25.0 ºC.

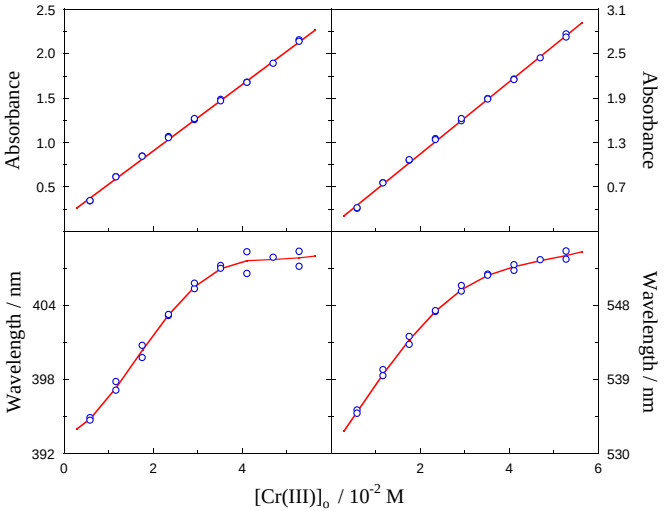

Figure 5. Wavelengths (bottom) and absorbances (top) corresponding to the first (left) and second (right) peaks of the electronic spectrum recorded for the final violet complex as a function of the metal ion initial concentration at $[Cr(NO_3)_3]_o$ = (0.59 – 5.29) × 10^{-2} M, [sodium hydrogen L-glutamate]$_o$ = 0.392 M, pH 4.68 – 5.75 and 25.0 ºC.

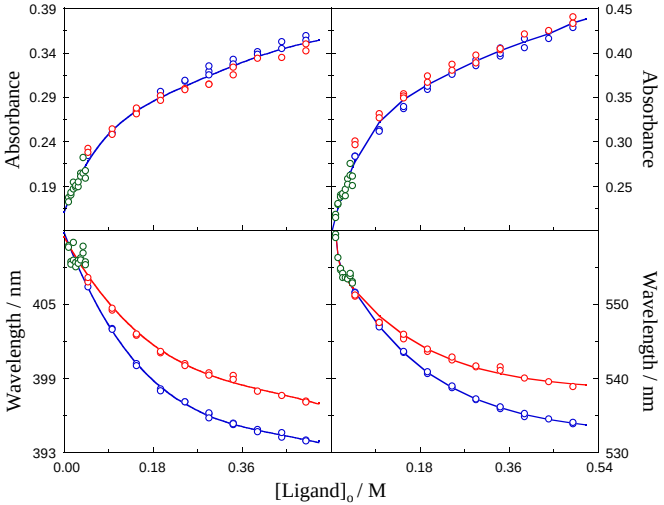

Figure 6. Wavelengths (bottom) and absorbances (top) corresponding to the first (left) and second (right) peaks of the electronic spectrum recorded for the final violet complex as a function of the organic ligand initial concentration at $[Cr(NO_3)_3]_o$ = 5.88 × 10^{-3} M and 25.0 ºC. Green points: [L-glutamic acid]$_o$ = (0.98 – 4.41) × 10^{-2} M, [KOH]$_o$ = 1.96 × 10^{-2} M, pH 3.37 – 3.88. Red points: [L-glutamic acid]$_o$ = 0.049 – 0.490 M, [KOH]$_o$ = 0.059 – 0.589 M, pH 4.43 – 5.01. Blue points: [sodium hydrogen L-glutamate]$_o$ = 0.049 – 0.490 M, pH 4.77 – 5.87.

The spectroscopic data shown in Figures 3-6 indicate that the first visible peak of the final reacting mixture lies in the range 394 – 410 nm, and the second in the range 534 – 568 nm, increasing both with the initial concentration of metal ion and decreasing both with the initial concentration of ligand.

Although the existence of only one complex of Cr(III) with L-glutamic acid has been reported (with the stoichiometric ratio 1 : 3 for metal ion : organic ligand),[23] the results shown in Figures 3-6 cannot be explained unless we assume the presence of at least two different complexes in the final reacting mixture. Thus, although the participation of other complexes cannot be discarded, the simplest explanation for the experimental data so far available is that two complexes differing only in the number of ligands coexist in equilibrium in the final reacting mixture:

$$C_n + Glu \overset{K}{\rightleftharpoons} C_{n+1} \qquad (1)$$

where C_n and C_{n+1} are Cr(III) complexes involving n and n+1 L-glutamic acid ligands, respectively. The corresponding equilibrium constant would be:

$$K = \frac{[C_{n+1}]}{[C_n]\,[Glu]} \qquad (2)$$

In writing eq 2, the approximate expression of the equilibrium constant referred to concentrations (in M^{-1}) has been preferred over the more exact referred to activities (dimensionless) because this is the approximation usually made in chemical kinetics.

Now, a matter balance for Cr(III) allows us to write:

$$[Cr(III)]_T = [C_n] + [C_{n+1}] = [C_n] + K\,[C_n]\,[Glu] \qquad (3)$$

where $[Cr(III)]_T$ stands for the total concentration of metal ion. From eqs 2 and 3, it follows that:

$$[C_n] = \frac{[Cr(III)]_T}{1 + K\,[Glu]} \qquad (4)$$

$$[C_{n+1}] = \frac{K\,[Cr(III)]_T\,[Glu]}{1 + K\,[Glu]} \qquad (5)$$

and from eqs 4 and 5:

$$\frac{[C_{n+1}]}{[C_n]} = K\,[Glu] \quad (6)$$

It should be observed that [Glu] represents the concentration of free L-glutamic acid. A matter balance for the organic reactant will allow us to evaluate how much of it is present in the free form and how much in the ligand form:

$$[Glu]_T = [Glu] + n[C_n] + (n+1)[C_{n+1}] \quad (7)$$

where $[Glu]_T$ stands for the total concentration of L-glutamic acid. From eqs 6 and 7:

$$\frac{[C_{n+1}]}{[C_n]} = K\left\{[Glu]_T - n[C_n] - (n+1)[C_{n+1}]\right\} \quad (8)$$

Since an increase of the metal ion initial concentration results in an increase of the concentrations of both complexes C_n and C_{n+1}, and so in a decrease of the concentration of the free amino acid (a decrease of the $[C_{n+1}]/[C_n]$ ratio), whereas an increase of the L-glutamic acid initial concentration leads to the opposite result (an increase of both the free amino acid concentration and the $[C_{n+1}]/[C_n]$ ratio), eq 8 is consistent with the plots shown in Figures 3-6 provided that the electronic spectra corresponding to the different complexes are shifted toward lower wavelengths as the number of organic ligands increases and, at the same time, there is an enhancement of the intensity of the absorption peaks:

$$\lambda_{1,2}(0) > \lambda_{1,2}(n) > \lambda_{1,2}(n+1) \quad (9)$$

$$\varepsilon_{1,2}(0) < \varepsilon_{1,2}(n) < \varepsilon_{1,2}(n+1) \quad (10)$$

In the inequalities written in eqs 9 and 10 the subscripts indicate that the wavelengths and molar absorption coefficients correspond to both peaks of the spectrum (the first and the second) and the quantities within parentheses stand for the number of organic ligands involved in each of the four complexes proposed: 0 for the initial inorganic reactant, either blue $[Cr(H_2O)_6]^{3+}$ or green $[Cr(OH)(H_2O)_5]^{2+}$, n for the final violet complex C_n and n+1 for the final violet complex C_{n+1}.

In addition, the finding of two different curves for the dependence of the wavelengths associated with both peaks of the final visible spectrum on the organic ligand initial concentration at different pH values (Figure 6 bottom, left and right) strongly suggests the existence of acid and base forms of the violet complex in equilibrium:

$$C_{n+1} + H^+ \rightleftharpoons C_{n+1} - H^+ \quad (11)$$

so that the corresponding wavelengths and molar absorption coefficients follow the sequences:

$$\lambda_{1,2}(C_{n+1}) < \lambda_{1,2}(C_{n+1} - H^+) \quad (12)$$

$$\varepsilon_{1,2}(C_{n+1}) \approx \varepsilon_{1,2}(C_{n+1} - H^+) \quad (13)$$

Equation 12 explains the behavior found in Figure 6 (bottom, left and right), whereas eq 13 explains that found in Figure 6 (top, left and right). Although eq 11 has been written for the complex with the highest number of organic ligands (C_{n+1}), the existence of a similar acid-base equilibrium for complex C_n cannot be discarded at all.

7. ABSORBANCE-TIME DATA

The absorbances at both 580 and 410 nm have been plotted against the absorbance at 545 nm during the course of the reaction for a typical kinetic run. It can be observed that the *A*(410) vs. *A*(545) plot is linear (Figure 7, bottom), whereas the *A*(580) vs. *A*(545) plot shows a downward-concave curvature (Figure 7, top). In order to understand this experimental behavior, let us start writing the total absorbance of the solution at each wavelength (λ_1 and λ_2) as a sum of the independent contributions of two chemical species, the blue-green Cr(III) complex acting as reactant (R) and the violet Cr(III) complex acting as product (P). Assuming that both species fulfill the Lambert-Beer law:

$$A(\lambda_1) = \varepsilon_{R,1}\, l\, [R] + \varepsilon_{P,1}\, l\, [P] \quad (14)$$

$$A(\lambda_2) = \varepsilon_{R,2}\, l\, [R] + \varepsilon_{P,2}\, l\, [P] \quad (15)$$

where the subscripts of the molar absorption coefficients (ε) correspond to each chemical species and wavelength, and l is the optical path length (1 cm).

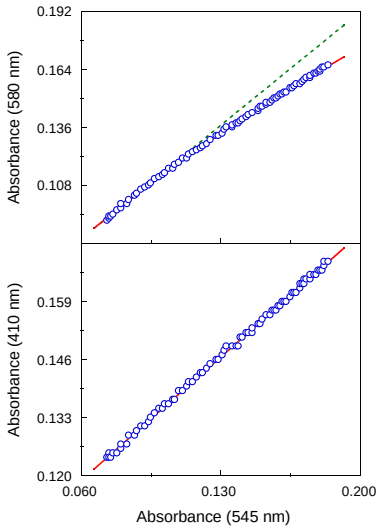

Figure 7. Absorbances at 580 (top) and 410 (bottom) nm as a function of the absorbance at 545 nm during the course of the reaction. The dashed line is the tangent to the curve at the beginning of the reaction. $[Cr(NO_3)_3]_o = 5.88 \times 10^{-3}$ M, [L-glutamic acid]$_o$ = 3.43×10^{-2} M, $[KOH]_o = 2.03 \times 10^{-2}$ M, pH 3.45, 25.0 ºC.

Considering now that all the possible intermediates are in steady state (reactive enough to be in negligible concentration),[30] a simple mass balance allows writing:

$$A(\lambda_1) = \varepsilon_{R,1}\, l\, ([R]_o - x) + \varepsilon_{P,1}\, l\, x \quad (16)$$

$$A(\lambda_2) = \varepsilon_{R,2}\, l\, ([R]_o - x) + \varepsilon_{P,2}\, l\, x \quad (17)$$

where x is the conversion variable (extent of reaction per unit volume) at a certain instant during the course of the process. From eq 17:

$$x = \frac{A(\lambda_2) - A(\lambda_2)_o}{(\varepsilon_{P,2} - \varepsilon_{R,2})\, l} \quad (18)$$

$A(\lambda_2)_o = \varepsilon_{R,2}\, l\, [R]_o$ being the initial absorbance of the solution at the second wavelength. Finally, from eqs 16 and 18:

$$A(\lambda_1) = A(\lambda_1)_o + \frac{\varepsilon_{P,1} - \varepsilon_{R,1}}{\varepsilon_{P,2} - \varepsilon_{R,2}} \left[A(\lambda_2) - A(\lambda_2)_o \right] \quad (19)$$

where $A(\lambda_1)_o = \varepsilon_{R,1}\, l\, [R]_o$ is the initial absorbance at the first wavelength. The only terms changing with time during the course of the reaction in eq 19 are $A(\lambda_1)$ and $A(\lambda_2)$, so that this equation predicts the existence of a linear correlation between the absorbances at two different wavelengths, in perfect agreement with the behavior observed in Figure 7 (bottom). However, the plot in Figure 7 (top) shows a certain downward-concave curvature. Given that the fulfillment of the Lambert-Beer law in diluted enough solutions is well established, it can be inferred that the mass balance used in eqs 16 and 17 should be corrected to include the involvement of at least one long-lived intermediate (I).

According to this interpretation, since the slope of the plot is constant during the course of the reaction when the 410-545 couple of wavelengths is chosen, we can conclude that the ratio of differences of molar absorption coefficients remains approximately unchanged when the reaction R→I is replaced by I→P:

$$\frac{\varepsilon_{I,410} - \varepsilon_{R,410}}{\varepsilon_{I,545} - \varepsilon_{R,545}} \approx \frac{\varepsilon_{P,410} - \varepsilon_{I,410}}{\varepsilon_{P,545} - \varepsilon_{I,545}} \quad (20)$$

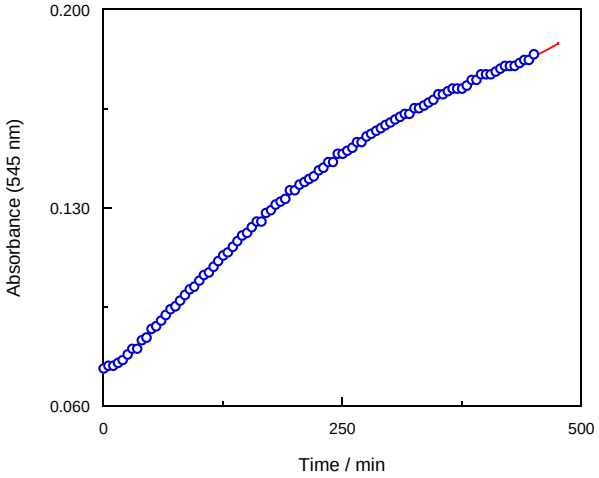

Figure 8. Absorbance at 545 nm as a function of time during the course of the reaction. $[Cr(NO_3)_3]_o$ = 5.88 × 10^{-3} M, $[L\text{-glutamic acid}]_o$ = 3.43 × 10^{-2} M, $[KOH]_o$ = 2.03 × 10^{-2} M, pH 3.45, 25.0 ºC.

Nevertheless, when the 580-545 wavelength couple is chosen the slope of the plot decreases gradually as the reaction advances, allowing us to infer that:

$$\frac{\varepsilon_{I,580} - \varepsilon_{R,580}}{\varepsilon_{I,545} - \varepsilon_{R,545}} > \frac{\varepsilon_{P,580} - \varepsilon_{I,580}}{\varepsilon_{P,545} - \varepsilon_{I,545}} \quad (21)$$

On the other hand, the absorbance-time plots showed in all cases a sigmoidal pattern, with an initial upward-concave stretch followed by an inflection point and a downward-concave stretch (Figure 8), typical of reactions with consecutive acceleration and deceleration periods.

8. TIME DEPENDENCE OF THE REACTION RATE

The values of the reaction rate can be obtained by means of the finite difference method. This mathematical procedure of approximate derivation allows the calculation of the rate at time $t + \Delta t/2$ from the product concentrations at times t and $t + \Delta t$ as:

$$v_t = \frac{d[P]_t}{dt} \approx \frac{c(t + \Delta t) - c(t)}{\Delta t} \quad (22)$$

Equation 22 leads to reaction rate values with a very low systematic error provided that the time interval chosen (Δt) is small enough, and its combination with the formula of the additive properties[31] leads to:

$$v_t \approx \frac{1}{A_\infty - A_o} \frac{A(t + \Delta t) - A(t)}{\Delta t} [R]_o \quad (23)$$

A_o, $A(t)$, $A(t + \Delta t)$ and A_∞ being the absorbances at times 0, t, $t + \Delta t$ and ∞, respectively, whereas $[R]_o$ stands for the initial concentration of the limiting reactant.

The reaction rate so obtained has been plotted against time for a typical kinetic run in Figure 9. It can be seen that the curve shows a definite bell-shaped pattern: the rate increases from the beginning of the reaction (acceleration period), reaches a maximum and then decreases (deceleration period). This peculiar kinetic behavior admits two alternative interpretations:

(i) When the reaction is monitored by following the decay of a reactant concentration (absorbance decreasing with time), a bell-shaped rate vs. time plot is indicative of an autocatalytic reaction.

(ii) When the reaction is monitored by following the formation of a product (absorbance increasing with time), a bell-shaped rate vs. time plot can be explained either by the presence of an autocatalytic phenomenon or by the involvement in the mechanism of a long-lived intermediate (not in steady state).

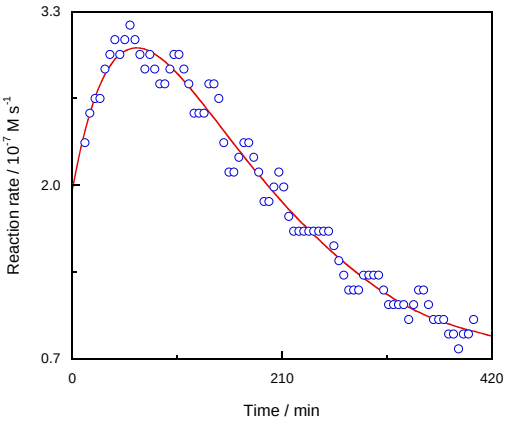

Figure 9. Reaction rate as a function of time for a typical kinetic run. $[Cr(NO_3)_3]_o = 5.88 \times 10^{-3}$ M, $[\text{L-glutamic acid}]_o = 3.92 \times 10^{-2}$ M, $[KOH]_o = 2.85 \times 10^{-2}$ M, pH 3.63, 25.0 ºC.

In the present case, we find ourselves in the second situation. Therefore, the two alternatives would be possible in principle. However, the autocatalytic behavior would be expected for reactions leading to especially reactive products (such as in ester hydrolyses autocatalyzed by acids[32] and permanganate oxidations of amino acids autocatalyzed by colloidal manganese dioxide[33]) or intermediates (such as in the chlorine dioxide-thiourea dioxide reaction[34]). Given the inherent inertness of the Cr(III) complexes, the explanation based on the long-lived intermediate seems much more likely to be correct, and it will be confirmed later by the excellent accordance between the experimental absorbance-time data and those derived from the proposed kinetic model.

9. TWO RATE CONSTANT KINETIC MODEL FOR THE REACTION

9.1. APPROXIMATE INTEGRATION: NUMERICAL SIMULATIONS

It has been demonstrated that, since the rate does not decrease exponentially with time, the Cr(III)-glutamic acid complexation cannot be considered as a pseudo-first order reaction, even under a ligand/metal ion large excess. Given the impossibility of obtaining good results in the fit of the experimental absorbance-time data when one rate constant kinetic models were used, several two rate constant models were tried. To that end, a numerical approximate integration method was used. The advantage of performing an approximate integration of the kinetic differential equations is that all the combinations of elementary reaction steps are possible, whereas the application of exact integration methods requires that all the steps involved in the mechanism be of first order (or, at least, of pseudo-first order).

The approximate integrations were done by means of the fourth-order Runge-Kutta method.[35] This numerical integration method was applied to different combinations of two elementary reaction steps, corresponding to the formation and disappearance of a long-lived intermediate, the first step of first order in the reactant Cr(III) and the second of first order in the intermediate, the combinations including zero order and first order dependences on the concentration of glutamic acid and, sometimes, a first order dependence on the concentration of hydroxide ion. The combination that seemed to fit best the experimental data was the simplest one, two consecutive first order elementary reactions according to the sequence:

$$\mathrm{R} \xrightarrow{k_1} \mathrm{I} \xrightarrow{k_2} \mathrm{P} \qquad (24)$$

The corresponding differential equations are:

$$\frac{\mathrm{d[R]}}{\mathrm{d}t} = -k_1\,[\mathrm{R}] \qquad (25)$$

$$\frac{\mathrm{d[I]}}{\mathrm{d}t} = k_1\,[\mathrm{R}] - k_2\,[\mathrm{I}] \qquad (26)$$

$$\frac{\mathrm{d[P]}}{\mathrm{d}t} = k_2\,[\mathrm{I}] \qquad (27)$$

and the reaction rate (defined from the time evolution of the product):

$$v = \frac{\mathrm{d[P]}}{\mathrm{d}t} = k_2\,[\mathrm{I}] \tag{28}$$

It can be seen that the kinetic differential equations associated with the chemical species consumed or formed in the elementary steps involved in the proposed mechanism (eqs 25-27) are of the following type:

$$\frac{\mathrm{d}c_{\mathrm{i},t}}{\mathrm{d}t} = f(c_{\mathrm{i},t}, c_{\mathrm{j},t}, ...) \tag{29}$$

$c_{\mathrm{i},t}$, $c_{\mathrm{j},t}$, ... standing for the concentrations of different chemical species (reactants, intermediates, products, catalysts or inhibitors) at the instant *t* during the course of the reaction. The approximate integrated form of eq 29 is:

$$c_{\mathrm{i},t} = c_{\mathrm{i},t-\Delta t} + \frac{1}{6}(a_{0,\mathrm{i}} + 2a_{1,\mathrm{i}} + 2a_{2,\mathrm{i}} + a_{3,\mathrm{i}}) \tag{30}$$

where Δt is the interval of time chosen to perform the integration. The smaller the interval the lower will be the error committed in the approximation, but the higher the computation time required to carrying out the calculations. The coefficients within parentheses are defined as:

$$a_{0,\mathrm{i}} = f(c_{\mathrm{i},t-\Delta t}, c_{\mathrm{j},t-\Delta t}, ...)\,\Delta t \tag{31}$$

$$a_{1,\mathrm{i}} = f(c_{\mathrm{i},t-\Delta t} + \frac{a_{0,\mathrm{i}}}{2}, c_{\mathrm{j},t-\Delta t} + \frac{a_{0,\mathrm{j}}}{2}, ...)\,\Delta t \tag{32}$$

$$a_{2,\mathrm{i}} = f(c_{\mathrm{i},t-\Delta t} + \frac{a_{1,\mathrm{i}}}{2}, c_{\mathrm{j},t-\Delta t} + \frac{a_{1,\mathrm{j}}}{2}, ...)\,\Delta t \tag{33}$$

$$a_{3,\mathrm{i}} = f(c_{\mathrm{i},t-\Delta t} + a_{2,\mathrm{i}}, c_{\mathrm{j},t-\Delta t} + a_{2,\mathrm{j}}, ...)\,\Delta t \tag{34}$$

The values of the rate constants involved in the differential expressions of the type shown in eq 29 were obtained by trying systematically many combinations until the best fit of the experimental data was found.

9.2. APPROXIMATE INTEGRATION: INTERMEDIATE IN STEADY STATE

Thus, the mechanism assumed to perform the kinetic calculations was constituted by two consecutive first-order elementary reactions. In the hypothetical case that the reaction intermediate be reactive enough, the steady state approximation would be applicable. To that

end, it is required that the intermediate in question be formed in a slow step and decayed in a fast step:

$$\mathrm{R} \xrightarrow[\text{slow}]{k_1} \mathrm{I} \xrightarrow[\text{fast}]{k_2} \mathrm{P} \tag{35}$$

From eq 26:

$$\frac{\mathrm{d[I]}}{\mathrm{d}t} = k_1\,[\mathrm{R}] - k_2\,[\mathrm{I}] \approx 0 \tag{36}$$

$$[\mathrm{I}] \approx \frac{k_1}{k_2}\,[\mathrm{R}] \tag{37}$$

and replacing into eq 28:

$$v \approx k_1\,[\mathrm{R}] \tag{38}$$

Hence, the simple mechanism constituted by two consecutive unimolecular reactions leads to a rate law of first order in the reactant provided that the intermediate involved be reactive enough to apply the steady state condition.

It is said in many chemical kinetics[36] or physical chemistry[37] textbooks that eq 36 is equivalent to accept that the steady state intermediates are in almost constant concentration. However, as pointed out already by some authors,[31] this interpretation is not correct. Effectively, integration of eq 25 leads to:

$$[\mathrm{R}] = [\mathrm{R}]_\mathrm{o}\, e^{-k_1 t} \tag{39}$$

and from eq 37:

$$[\mathrm{I}] \approx \frac{k_1}{k_2}\,[\mathrm{R}]_\mathrm{o}\, e^{-k_1 t} \tag{40}$$

It can then be concluded that, for the particular mechanism considered, the concentration of the intermediate in steady state decreases exponentially with time, in open contradiction with the constant concentration hypothesis. This approximation can be applied only to very reactive intermediates, present in minute concentration, and only once their maximum concentration is reached, so that they can decay at the same rhythm as the limiting reactant does.

9.3. EXACT INTEGRATION: INTERMEDIATE NOT IN STEADY STATE

Since the experimental data available for the Cr(III)-glutamic acid reaction do not follow the kinetic model predicted by eq 38, it cannot be of first order in the inorganic reactant (even under

a large excess of ligand). Therefore, it can be concluded that the intermediate involved in the mechanism is too long-lived to be in steady state, the slow step being probably the one corresponding to its decay:

$$\mathrm{R} \xrightarrow[\text{fast}]{k_1} \mathrm{I} \xrightarrow[\text{slow}]{k_2} \mathrm{P} \tag{41}$$

and consequently, eq 26 must be integrated to obtain an exact solution. Given the impossibility of separating variables (intermediate concentration and time), the integration must be performed by means of a matrix method.[38] The resulting equation, that can be consulted in many textbooks,[39] is the following:

$$[\mathrm{I}] = \frac{k_1 [\mathrm{R}]_\mathrm{o}}{k_2 - k_1} (e^{-k_1 t} - e^{-k_2 t}) \tag{42}$$

whereas the temporal dependence of the product concentration can be obtained from those corresponding to the reactant (eq 39) and intermediate (eq 42) by means of the mass balance:

$$[\mathrm{P}] = [\mathrm{R}]_\mathrm{o} - [\mathrm{R}] - [\mathrm{I}] \tag{43}$$

The total absorbance of the reacting mixture as a certain wavelength can be deduced by application of the Beer-Lambert law to the three Cr(III) complexes involved (reactant, long-lived intermediate and product):

$$A_\lambda = (\varepsilon_{\mathrm{R},\lambda} [\mathrm{R}] + \varepsilon_{\mathrm{I},\lambda} [\mathrm{I}] + \varepsilon_{\mathrm{P},\lambda} [\mathrm{P}]) l \tag{44}$$

where $\varepsilon_{\mathrm{R},\lambda}$, $\varepsilon_{\mathrm{I},\lambda}$ and $\varepsilon_{\mathrm{P},\lambda}$ are the respective molar absorption coefficients and l = 1 cm is the optical path length. The values of $\varepsilon_{\mathrm{R},\lambda}$ and $\varepsilon_{\mathrm{P},\lambda}$ are related to the initial and final absorbances as:

$$\varepsilon_{\mathrm{R},\lambda} = \frac{A_{\lambda,0}}{[\mathrm{R}]_\mathrm{o} l} \tag{45}$$

$$\varepsilon_{\mathrm{P},\lambda} = \frac{A_{\lambda,\infty}}{[\mathrm{R}]_\mathrm{o} l} \tag{46}$$

having been considered that the final concentration of the product equals the initial concentration of the limiting reactant, once the latter species and the long-lived intermediate are both exhausted. In order to estimate the contribution of the intermediate to the total optical

density of the reacting mixture, a new parameter had to be introduced into the calculations, corresponding to the ratio between its molar absorption coefficient and that of the reactant:

$$Q = \frac{\varepsilon_{\mathrm{I},\lambda}}{\varepsilon_{\mathrm{R},\lambda}} \tag{47}$$

Two computer programs have been written in BASIC language to perform the required calculations. In program I, different values of five fitting parameters ($A_{\lambda,0}$, $A_{\lambda,\infty}$, k_1, k_2 and Q) were systematically varied until the best fit was found. This was defined as the one that minimized the average error given by:

$$E = \frac{\sum_{\mathrm{i}=1}^{N} \left| A_{\mathrm{i,cal}} - A_{\mathrm{i,exp}} \right|}{N} \tag{48}$$

where $A_{\mathrm{i,cal}}$ and $A_{\mathrm{i,exp}}$ are the calculated and experimental values of the absorbance at different instants during the course of the reaction, respectively, and N is the number of absorbance-time couples of experimental data recorded for each kinetic run. This program was applied to two independent kinetic runs, leading to the value Q = 1.089 ± 0.009.

With the objective of decreasing the accidental errors as much as possible, a second program was written using only four fitting parameters ($A_{\lambda,0}$, $A_{\lambda,\infty}$, k_1 and k_2) and keeping constant the value of parameter Q given above. Program II yielded an excellent concordance between the theoretical and experimental absorbances. Depending on the experimental conditions, the average error spanned within the range E = 2.94×10^{-4} to 1.65×10^{-3}.

It should be observed that the particular mechanism given by eq 41 can be resolved by the Runge-Kutta approximate method of numerical integration (eqs 30-34) or by the exact integration method (eqs 39, 42 and 43), both procedures yielding almost identical results for the rate constants.

10. KINETIC RESULTS

The reaction rate is always a function of several variables. In the case of the Cr(III)-glutamic acid complexation, the dependences of the rate on the initial concentrations of metal ion and ligand, ionic strength, pH and temperature are of special interest. In order to make easier the analysis of the results, it is the usual procedure in chemical kinetics to organize the experiments in several series, isolating one of the variables in each series and keeping all the others constant whenever possible. In the present study, this method has been applied, although in some series the pH changed as the initial concentrations of Cr(III), L-glutamic acid or sodium hydrogen L-glutamate varied. This circumstance has been taken into account in the interpretation of the kinetic data obtained in the laboratory. Besides the change in pH from one experiment to another within certain series of experiments, it is necessary to consider the pH decrease during each kinetic run due to the release of hydrogen ions from glutamic acid to the medium as the complexation of Cr(III) by its ligand advances. The use of a buffer mixture is contraindicated in this particular reaction because of the possibility of its anionic form (or forms) acting as a competing ligand for the metal ion.

10.1. EFFECT OF THE INITIAL METAL ION CONCENTRATION

A series of kinetic runs was performed at different initial Cr(III) concentrations, all the other experimental conditions remaining constant. The results are shown in Table 1. A double-logarithm plot of rate constant k_1 against the metal ion initial concentration yielded a straight line with slope -0.48 ± 0.04, whereas the slope of the corresponding plot for rate constant k_2 was -0.04 ± 0.07 (Figure 10, left). Since true rate constants should not depend on the initial concentration of Cr(III), the results found for the second rate constant have to be considered excellent (although very scattered due to accidental errors). In the case of the first rate constant, however, the results show the existence of a systematic error caused by the change in the reacting mixture pH. Effectively, as we will see later, the reaction presents base catalysis and, since L-glutamic acid must release hydrogen ions to the medium in order to complex the metal ion, the pH decreases as the reaction advances, and this decrease is more intense at high Cr(III) initial concentrations than at low ones, thus explaining the negative value of the slope of the double-logarithm plot.

$[Cr(NO_3)_3]_o$ [10^{-2} M]	pH	k_1 [10^{-4} s^{-1}]	k_2 [10^{-5} s^{-1}]	E [10^{-4}]
0.29	3.57 ± 0.03	2.22 ± 0.51	4.84 ± 1.18	3.93 ± 0.11
0.59	3.29 ± 0.01	3.21 ± 0.70	2.85 ± 0.51	3.57 ± 0.64
0.88	3.02 ± 0.08	2.22 ± 0.40	3.86 ± 0.40	4.49 ± 0.38
1.18	2.93 ± 0.07	1.64 ± 0.25	3.24 ± 0.57	4.58 ± 0.54
1.47	2.84 ± 0.07	1.77 ± 0.25	3.21 ± 0.51	3.83 ± 0.12
1.76	2.78 ± 0.07	1.45 ± 0.09	3.43 ± 0.10	3.51 ± 0.39
2.06	2.73 ± 0.06	1.38 ± 0.05	2.49 ± 0.39	3.46 ± 0.15
2.35	2.67 ± 0.07	1.31 ± 0.10	3.28 ± 0.29	3.29 ± 0.24
2.65	2.62 ± 0.04	1.27 ± 0.10	2.28 ± 0.63	4.66 ± 1.46
2.94	2.58 ± 0.04	1.11 ± 0.09	2.75 ± 1.08	3.70 ± 0.35
3.23	2.55 ± 0.03	1.05 ± 0.05	2.96 ± 0.06	3.59 ± 0.02
3.53	2.51 ± 0.02	1.02 ± 0.01	4.71 ± 0.02	5.26 ± 1.07
3.82	2.48 ± 0.01	1.04 ± 0.04	2.46 ± 0.36	3.70 ± 0.51
4.12	2.46 ± 0.01	0.92 ± 0.02	3.27 ± 0.43	3.58 ± 0.05

(a) The pH values were measured at the end of the reaction.
(b) *E* is the average error of the theoretical absorbances with respect to the experimental ones.

Table 1. Experimental rate constants at different initial metal ion concentrations. [L-glutamic acid]$_o$ = 3.92 × 10^{-2} M, [KOH]$_o$ = 1.62 × 10^{-2} M, 25.0 ºC.

The existence of systematic errors yielding rate constants dependent on the initial concentration of the limiting reactant is rather frequent in experimental chemical kinetics, especially in those cases where two[28,40,41] or more[33] rate constants are needed to fit the absorbance-time data.

The effect of the initial concentration of metal ion on the reaction rate was studied again under different experimental conditions, using this time sodium hydrogen L-glutamate instead of L-glutamic acid as organic ligand. The values obtained for the corresponding experimental rate constants appear compiled in Table 2, and have been plotted as double-logarithm linear representations in Figure 10 (right). It can be observed that both k_1 and k_2 decreased with increasing initial concentration of Cr(III), the respective slopes being -0.48 ± 0.02 and -0.45 ± 0.01.

$[Cr(NO_3)_3]_o$ [10^{-2} M]	pH	k_1 [10^{-2} s^{-1}]	k_2 [10^{-3} s^{-1}]	E [10^{-4}]
0.59	5.754 ± 0.006	1.77 ± 0.04	2.82 ± 0.03	6.80 ± 0.04
1.18	5.468 ± 0.006	1.28 ± 0.07	1.99 ± 0.02	5.06 ± 0.51
1.76	5.283 ± 0.005	1.01 ± 0.02	1.63 ± 0.03	4.08 ± 0.25
2.35	5.137 ± 0.001	0.92 ± 0.05	1.44 ± 0.02	3.95 ± 0.36
2.94	5.031 ± 0.002	0.73 ± 0.04	1.24 ± 0.04	3.67 ± 0.28
3.53	4.934 ± 0.007	0.73 ± 0.01	1.17 ± 0.02	3.36 ± 0.06
4.12	4.851 ± 0.007	0.73 ± 0.04	1.10 ± 0.01	3.34 ± 0.05
4.71	4.762 ± 0.002	0.67 ± 0.01	1.04 ± 0.01	3.38 ± 0.21
5.29	4.682 ± 0.004	0.60 ± 0.02	1.04 ± 0.02	3.91 ± 0.17
5.88	4.609 ± 0.004	0.58 ± 0.02	0.98 ± 0.01	3.61 ± 0.05
6.47	4.529 ± 0.004	0.55 ± 0.01	0.99 ± 0.01	3.48 ± 0.27

(a) The pH values were measured at the end of the reaction.
(b) *E* is the average error of the theoretical absorbances with respect to the experimental ones.

Table 2. Experimental rate constants at different initial metal ion concentrations. [Sodium hydrogen L-glutamate]$_o$ = 0.392 M, 25.0 ºC.

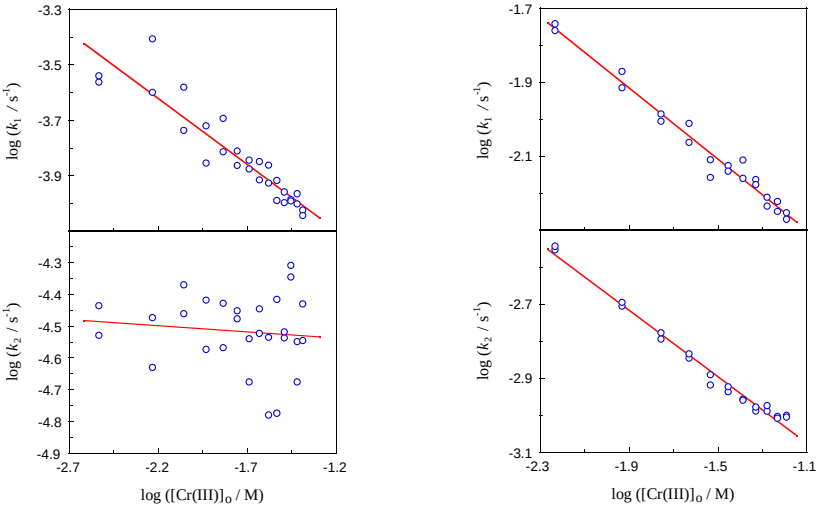

Figure 10. Dependence of the experimental rate constants on the initial concentration of metal ion at 25.0 ºC. Left: $[Cr(NO_3)_3]_o$ = (0.29 – 4.12) × 10^{-2} M, [L-glutamic acid]$_o$ = 3.92 × 10^{-2} M, $[KOH]_o$ = 1.62 × 10^{-2} M, pH 2.46 – 3.57, r = 0.928 (top) and 0.111 (bottom). Right: $[Cr(NO_3)_3]_o$ = (0.59 – 6.47) × 10^{-2} M, [sodium hydrogen L-glutamate]$_o$ = 0.392 M, pH 4.53 – 5.75, r = 0.987 (top) and 0.992 (bottom).

10.2. EFFECT OF THE INITIAL LIGAND CONCENTRATION

In a series of kinetic experiments at gradually increasing initial concentration of L-glutamic acid and constant concentration of KOH both k_1 and k_2 decreased (Table 3). A double-logarithm plot of the rate constant against the ligand initial concentration yielded an upward-concave curve in the two cases (Figure 11). This unusual decrease of the rate constants as the initial concentration of a certain reactant increases can be explained by the parallel decrease of pH as the initial concentration of L-glutamic acid increased. Thus, because of this behavior, the study of the effect of the initial concentration of ligand on the reaction rate was repeated using this time sodium hydrogen L-glutamate instead of L-glutamic acid as reactant. Given that the pH values in this series of experiments was rather high, addition of KOH was no longer required. The results are shown in Table 4.

[L-glutamic acid]$_o$ [10^{-2} M]	pH	k_1 [10^{-3} s^{-1}]	k_2 [10^{-4} s^{-1}]	E [10^{-4}]
0.98	3.88 ± 0.01	9.46 ± 0.64	3.00 ± 0.20	14.17 ± 2.29
1.47	3.69 ± 0.01	2.01 ± 0.38	1.65 ± 0.02	5.92 ± 4.44
1.96	3.61 ± 0.01	1.00 ± 0.07	0.98 ± 0.03	4.68 ± 0.64
2.45	3.59 ± 0.02	0.58 ± 0.02	0.84 ± 0.03	3.21 ± 0.10
2.94	3.53 ± 0.04	0.47 ± 0.02	0.65 ± 0.01	4.27 ± 0.56
3.43	3.45 ± 0.01	0.41 ± 0.05	0.58 ± 0.02	4.27 ± 0.31
3.92	3.40 ± 0.04	0.37 ± 0.01	0.43 ± 0.02	3.91 ± 0.04
4.41	3.39 ± 0.02	0.35 ± 0.01	0.46 ± 0.02	3.70 ± 0.05

(a) The pH values were measured at the end of the reaction.
(b) *E* is the average error of the theoretical absorbances with respect to the experimental ones.

Table 3. Experimental rate constants at different L-glutamic acid initial concentrations. $[Cr(NO_3)_3]_o = 5.88 \times 10^{-3}$ M, $[KOH]_o = 1.96 \times 10^{-2}$ M, 25.0 ºC.

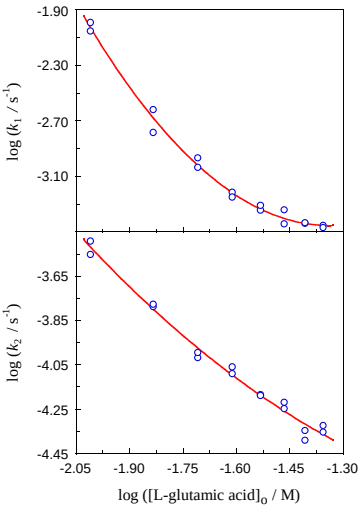

Figure 11. Dependence of the experimental rate constants k_1 (top) and k_2 (bottom) on the initial concentration of L-glutamic acid. $[Cr(NO_3)_3]_o = 5.88 \times 10^{-3}$ M, [L-glutamic acid]$_o$ = (0.98 – 4.41) $\times 10^{-2}$ M, $[KOH]_o = 1.96 \times 10^{-2}$ M, pH 3.37 – 3.88, 25.0 ºC.

$[L\text{-glutamate ion}]_o$ [M]	pH	k_1 [10^{-2} s^{-1}]	k_2 [10^{-3} s^{-1}]	E [10^{-4}]
0.049	4.773 ± 0.003	0.31 ± 0.02	0.42 ± 0.01	3.75 ± 0.01
0.098	5.134 ± 0.001	0.56 ± 0.06	0.86 ± 0.06	3.66 ± 0.03
0.147	5.321 ± 0.005	0.77 ± 0.01	1.19 ± 0.03	4.46 ± 0.52
0.196	5.451 ± 0.005	1.00 ± 0.04	1.62 ± 0.02	4.27 ± 0.46
0.245	5.550 ± 0.004	1.05 ± 0.07	2.03 ± 0.01	3.97 ± 0.01
0.294	5.626 ± 0.008	1.32 ± 0.14	2.43 ± 0.06	4.66 ± 0.26
0.343	5.700 ± 0.001	1.51 ± 0.08	2.75 ± 0.03	5.72 ± 1.03
0.392	5.754 ± 0.006	1.77 ± 0.04	2.82 ± 0.03	6.80 ± 0.04
0.441	5.810 ± 0.006	2.21 ± 0.05	2.88 ± 0.09	6.25 ± 2.35
0.490	5.865 ± 0.005	2.47 ± 0.26	3.56 ± 0.04	7.79 ± 3.07

(a) The pH values were measured at the end of the reaction.
(b) *E* is the average error of the theoretical absorbances with respect to the experimental ones.

Table 4. Experimental rate constants at different sodium hydrogen L-glutamate initial concentrations. $[Cr(NO_3)_3]_o = 5.88 \times 10^{-3}$ M, 25.0 ºC.

It can be observed that an increase of the initial concentration of organic ligand in the form of L-glutamate ion, unlike when it is used in the form of L-glutamic acid, results in an increase of the two experimental rate constants. The corresponding double-logarithm plots are linear (Figure 12, left) with the slopes 0.87 ± 0.03 (for k_1) and 0.91 ± 0.02 (for k_2). The finding of fractional values for these kinetic orders (not directly interpretable from the point of view of the mechanism) suggests that the correct rate law might be one of the saturation type, including the concentration of organic ligand in the numerator and again, within a sum, in the denominator. This kind of law has often been reported not only in complexation reactions,[28] but also when acid-base equilibria[42] or heterogeneous processes[43,44] are involved.

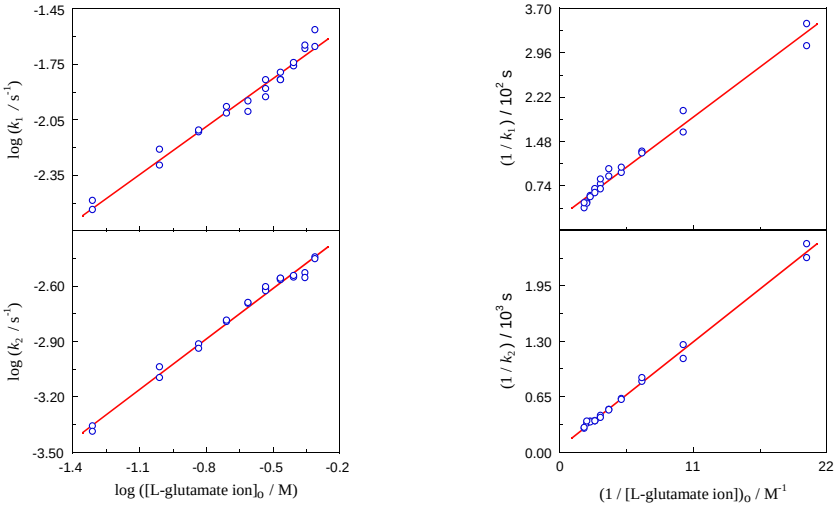

Figure 12. Effect of the initial concentration of organic ligand on the experimental rate constants at $[Cr(NO_3)_3]_o$ = 5.88 × 10^{-3} M, [sodium hydrogen L-glutamate]$_o$ = 0.049 – 0.490 M, pH 4.77 – 5.87 and 25.0 ºC. Left: double-logarithm dependence, r = 0.987 (top) and r = 0.994 (bottom). Right: double-reciprocal dependence, r = 0.990 (top) and r = 0.998 (bottom).

Therefore, the data compiled in Table 4, have been represented again in the form of double-reciprocal linear plots (Figure 12, right). It can be observed that the new plots are reasonably linear, with positive values for the corresponding intercepts and slopes. This is consistent with the fractional apparent kinetic orders found for glutamate ion from the correlations presented in Figure 12 (left).

10.3. EFFECT OF THE IONIC STRENGTH

The ionic strength of the medium was changed by the use of KNO_3 as background electrolyte, and its effect on the experimental rate constants has been compiled in Table 5. A plot of the logarithm of each rate constant against $I^{1/2}/(1+I^{1/2})$ yielded straight lines with the slopes – 0.41 ± 0.17 (for k_1) and 1.00 ± 0.29 (for k_2) $M^{-1/2}$ (Figure 13). This double dependence on the medium ionic strength (k_1 decreasing and k_2 increasing) matched the behavior reported for the Cr(III)-EDTA complexation reaction.[28]

[KNO_3] [M]	Ionic strength [M]	pH	k_1 [10^{-4} s^{-1}]	k_2 [10^{-5} s^{-1}]	E [10^{-4}]
0.000	0.051	3.29 ± 0.01	2.83 ± 0.31	2.83 ± 0.47	3.75 ± 0.96
0.059	0.110	3.24 ± 0.04	2.38 ± 0.01	3.01 ± 0.12	3.60 ± 0.09
0.118	0.169	3.25 ± 0.01	2.39 ± 0.05	3.09 ± 0.11	3.80 ± 0.07
0.176	0.228	3.23 ± 0.01	2.22 ± 0.05	3.09 ± 0.13	3.99 ± 0.02
0.235	0.287	3.26 ± 0.01	2.50 ± 0.21	3.09 ± 0.02	3.78 ± 0.20
0.294	0.345	3.33 ± 0.05	2.52 ± 0.01	4.42 ± 0.69	4.08 ± 0.48
0.353	0.404	3.34 ± 0.01	2.02 ± 0.03	4.83 ± 0.12	4.38 ± 0.07

(a) The pH values were measured at the end of the reaction.
(b) E is the average error of the theoretical absorbances with respect to the experimental ones.

Table 5. Experimental rate constants at different concentrations of potassium nitrate. $[Cr(NO_3)_3]_o = 5.88 \times 10^{-3}$ M, $[\text{L-glutamic acid}]_o = 3.92 \times 10^{-2}$ M, $[KOH]_o = 1.62 \times 10^{-2}$ M, 25.0 ºC.

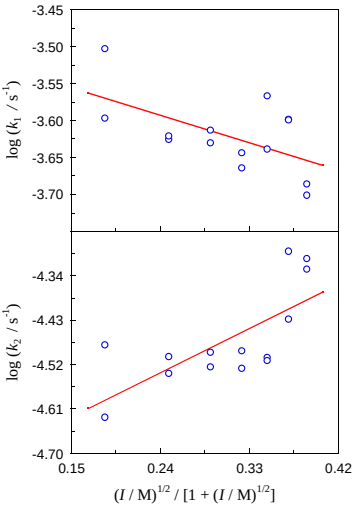

Figure 13. Dependence of the experimental rate constants k_1 (top, $r = 0.576$) and k_2 (bottom, $r = 0.711$) on the ionic strength. $[Cr(NO_3)_3]_o = 5.88 \times 10^{-3}$ M, $[\text{L-glutamic acid}]_o = 3.92 \times 10^{-2}$ M, $[KOH]_o = 1.62 \times 10^{-2}$ M, pH 3.20 – 3.38, 25.0 ºC.

10.4. EFFECT OF THE PH

The pH of the medium was varied by means of a changing concentration of KOH. An increase of the pH resulted in an increase of both k_1 and k_2 (Table 6), meaning that both steps presented base catalysis.

pH	k_1 [10^{-3} s^{-1}]	k_2 [10^{-4} s^{-1}]	E [10^{-4}]
3.288 ± 0.004	0.32 ± 0.07	0.28 ± 0.05	3.57 ± 0.64
3.400 ± 0.026	0.36 ± 0.01	0.43 ± 0.02	4.29 ± 0.40
3.533 ± 0.003	0.53 ± 0.05	0.70 ± 0.08	4.42 ± 0.67
3.651 ± 0.018	0.56 ± 0.04	0.81 ± 0.11	3.67 ± 0.20
3.812 ± 0.018	0.81 ± 0.09	1.14 ± 0.04	4.85 ± 0.07
3.954 ± 0.010	1.35 ± 0.02	1.51 ± 0.07	4.80 ± 0.41
4.099 ± 0.005	2.03 ± 0.36	2.18 ± 0.17	4.78 ± 0.08

(a) The pH values were measured at the end of the reaction.
(b) E is the average error of the theoretical absorbances with respect to the experimental ones.

Table 6. Experimental rate constants at different pH values. $[Cr(NO_3)_3]_o$ = 5.88 × 10^{-3} M, $[\text{L-glutamic acid}]_o$ = 3.92 × 10^{-2} M, $[KOH]_o$ = (1.59 – 4.07) × 10^{-2} M, 25.0 ºC.

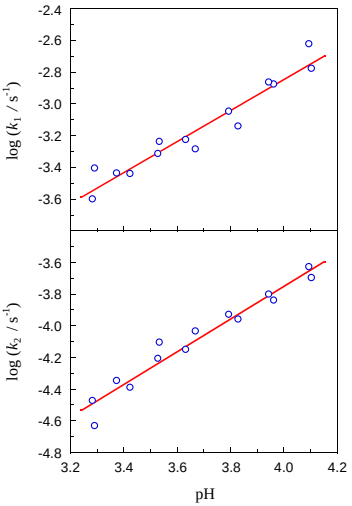

Figure 14. Dependence of the experimental rate constants k_1 (top, r = 0.964) and k_2 (bottom, r = 0.976) on the final pH. $[Cr(NO_3)_3]_o$ = 5.88 × 10^{-3} M, $[\text{L-glutamic acid}]_o$ = 3.92 × 10^{-2} M, $[KOH]_o$ = (1.59 – 4.07) × 10^{-2} M, 25.0 ºC.

The logarithms of the rate constants have been represented against the pH in Figure 14. We may observe that both plots are linear, and the slopes are 0.98 ± 0.08 (for k_1) and 1.03 ± 0.07 (for k_2). It can then be concluded that the two steps are of first order in hydroxide ion.

10.5. EFFECT OF TEMPERATURE

The experimental rate constants increased with increasing temperature in the range 15.0-25.0 ºC (Table 7).

Temperature [ºC]	k_1 [10^{-3} s^{-1}]	k_2 [10^{-4} s^{-1}]	E [10^{-4}]
15.0	0.61 ± 0.02	0.57 ± 0.05	4.54 ± 0.15
17.5	0.98 ± 0.03	0.82 ± 0.01	3.94 ± 0.12
20.0	0.98 ± 0.05	1.10 ± 0.06	4.67 ± 0.28
22.5	1.61 ± 0.19	1.52 ± 0.06	4.85 ± 0.07
25.0	2.03 ± 0.36	2.18 ± 0.17	4.78 ± 0.08

(a) E is the average error of the theoretical absorbances with respect to the experimental ones.

Table 7. Experimental rate constants at different temperatures. $[Cr(NO_3)_3]_o = 5.88 \times 10^{-3}$ M, [L-glutamic acid]$_o = 3.92 \times 10^{-2}$ M, $[KOH]_o = 4.05 \times 10^{-2}$ M, pH 4.09 ± 0.02.

In both cases the data were fitted by least squares to the Arrhenius equation:

$$k = A\, e^{-\frac{E_a}{RT}} \tag{49}$$

where A is the pre-exponential factor, E_a the activation energy, R the gas constant and T the absolute temperature. In addition, the temperature dependence of the rate constants can be described, as an alternative to the Arrhenius law, by means of the Eyring equation:

$$k = \kappa \frac{k_B T}{h} (c^o)^{1-n}\, e^{\frac{\Delta S^o_{\neq}}{R}}\, e^{-\frac{\Delta H^o_{\neq}}{RT}} \tag{50}$$

k_B and h being respectively the Boltzmann and Plank constants, c^o the standard concentration (1 mol L^{-1}), $\Delta S^o_{\ddagger}$ the activation entropy and $\Delta H^o_{\ddagger}$ the activation enthalpy. Parameter κ is the transmission coefficient (the probability of the activated complex breaking down into the reaction products) and, given our lack of knowledge about its value, is usually taken as unity. Equation

50 was originally written without the standard concentration factor, but it was introduced later to assume its dimensional homogeneity.[45]

The linear plots corresponding to the fitting of the rate constant-temperature data to the Arrhenius equation have been represented in Figure 15.

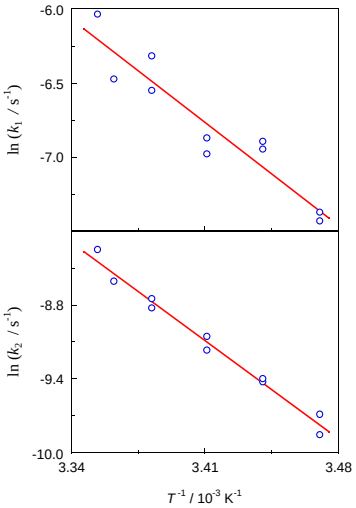

Figure 15. Arrhenius plots for the experimental rate constants k_1 (top, r = 0.944) and k_2 (bottom, r = 0.991). $[Cr(NO_3)_3]_o$ = 5.88 × 10^{-3} M, [L-glutamic acid]$_o$ = 3.92 × 10^{-2} M, $[KOH]_o$ = 4.05 × 10^{-2} M, pH 4.09 ± 0.02, 15.0 – 25.0 ºC.

The activation energies associated to rate constants k_1 and k_2 were obtained from the Arrhenius ln k vs. 1/T linear plots, whereas the corresponding activation enthalpies and entropies were deduced from the respective Eyring ln (k/T) vs. 1/T linear plots. The results are shown in Table 8.

Rate constant	E_a [kJ mol^{-1}]	$\Delta H^{o}_{\neq}$ [kJ mol^{-1}]	$\Delta S^{o}_{\neq}$ [J K^{-1} mol^{-1}]
k_1	83 ± 10	80 ± 10	- 27 ± 35
k_2	95 ± 5	92 ± 5	- 6 ± 15

(a) Errors associated to the activation parameters were calculated from the standard deviations for the intercepts and slopes of the Arrhenius and Eyring plots.

Table 8. Activation parameters associated to the experimental rate constants. $[Cr(NO_3)_3]_o$ = 5.88 × 10^{-3} M, [L-glutamic acid]$_o$ = 3.92 × 10^{-2} M, $[KOH]_o$ = 4.05 × 10^{-2} M, pH 4.09 ± 0.02, 15.0 – 25.0 ºC.

It can be observed that the activation energy associated to k_2 is higher than that associated to k_1, what is consistent with the previous assumption of the second step being the slow one (eq 41). The high values of these activation energies can be directly related to the remarkable inertness to substitution of the Cr(III) complexes, and are very close to the values found for the Cr(III)-EDTA reaction.[28] The activation entropies are both negative (activated complexes presumably more ordered than reactants), although the large uncertainties of these parameters do not allow to exclude the possibility of positive values. These uncertainties derive from the difficulty of extrapolating the values of the rate constants till infinite temperature, since $\Delta S^{o}_{\neq}$ is directly proportional to the logarithm of the Arrhenius pre-exponential factor,[46] that is:

$$\Delta S^{o}_{\neq} = R \ln \left[\frac{h A}{e\, k_B T_m (c^o)^{1-n}} \right] \quad (51)$$

and, according to the Arrhenius equation (eq 49), the pre-exponential factor is the value of the rate constant at infinite temperature:

$$\lim_{T \to \infty} k = A \quad (52)$$

11. MECHANISM

A qualitative energy-reaction coordinate diagram has been represented for the reaction (Figure 16).

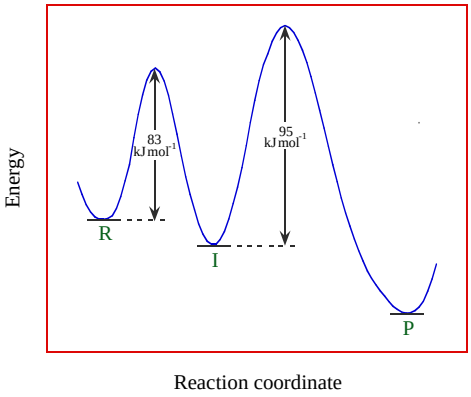

Figure 16. Qualitative energy-reaction coordinate diagram for the complexation of Cr(III) by L-glutamic acid showing the experimental activation energies corresponding to the conversions of the initial reactant (R) into the long-lived intermediate (I) and of the latter into the final product (P).

In order to draw the former diagram, it has been taken into account that the kinetic data obtained in the laboratory for the Cr(III)-glutamic acid complexation indicated that the first experimental rate constant (k_1) is one order of magnitude higher than the second (k_2), and the corresponding activation energies are coherent with these results ($E_{a,1} < E_{a,2}$). Thus, the step leading to the formation of the intermediate is fast whereas that leading to its decay is slow, what certainly explains the long-lived nature of that intermediate.

The mechanism that can be proposed for the first part of the complexation (from the reactants to the long-lived intermediate) consists of the following elementary steps:

$$[Cr(H_2O)_6]^{3+} \quad \overset{K_I}{\rightleftharpoons} \quad [Cr(OH)(H_2O)_5]^{2+} + H^+ \qquad (53)$$

$$[Cr(OH)(H_2O)_5]^{2+} \quad \underset{k_{-II}}{\overset{k_{II}\,(slow)}{\rightleftharpoons}} \quad [Cr(OH)(H_2O)_4]^{2+} + H_2O \qquad (54)$$

$$[Cr(OH)(H_2O)_4]^{2+} + HY^- \quad \xrightarrow{k_{III}} \quad [Cr(OH)(HY)(H_2O)_4]^{+} \qquad (55)$$

$$[Cr(OH)(HY)(H_2O)_4]^{+} + H^+ \quad \longrightarrow \quad [Cr(HY)(H_2O)_4]^{2+} + H_2O \qquad (56)$$

where HY^- stands for hydrogen L-glutamate ion. The experimental results show that the reaction rate presents a much stronger dependence on the concentration of hydroxide ion than on that of the organic ligand. This seems to suggest that the deprotonation associated with the observed base catalysis happens in a previous step, independent of the coordination of the ligand to the metal ion. Consequently, the proposed reaction sequence starts with the well-known acid-base equilibrium of hexaaquachromium(III) ion to yield hydroxopentaaquachromium(III) ion (eq 53, pK_a 4.29).[47,48] The presence of an OH^- ligand in the hydroxo complex renders the Cr(III)-H_2O chemical bonds more labile. The breakage of one of those bonds as in eq 54 has been postulated to be a requirement for the formation of the Cr(III)-EDTA complex.[27] Then, a competition between water (reverse direction of eq 54) and the organic ligand (HY^-, eq 55) for the vacant coordination site of the metal ion takes place, leading to the formation of the long-lived intermediate.

Assuming that the penta-coordinated intermediate is reactive enough to be in steady state (in other words, that it is formed in the slow step), and applying to eq 53 the quasi-equilibrium approximation, the following expression can be obtained for the first experimental rate constant:

$$k_1 = \frac{K_I\ k_{II}\ k_{III}\ [HY^-]}{(k_{-II} + k_{III}\ [HY^-])\ [H^+]} \quad (57)$$

Equation 57 is consistent with the results corresponding to the dependences of k_1 on the initial concentrations of organic ligand (Figure 12, right, top) and hydrogen ion (Figure 14, top). Moreover, the decreasing effect of the ionic strength (Figure 13, top) can be explained by the associated decrease of equilibrium constant K_I, since the reverse direction of eq 53 involves two like-charged ions as reactants.

On the other hand, the mechanism that can be proposed for the second part of the complexation (from the long-lived intermediate to the reaction product) is:

$$[Cr(HY)(H_2O)_4]^{2+} \xrightleftharpoons{K_{IV}} [Cr(OH)(HY)(H_2O)_3]^{+} + H^{+} \quad (58)$$

$$[Cr(OH)(HY)(H_2O)_3]^{+} \underset{k_{-V}}{\overset{k_{V}\ (slow)}{\rightleftharpoons}} [Cr(OH)(HY)(H_2O)_2]^{+} + H_2O \quad (59)$$

$$[Cr(OH)(HY)(H_2O)_2]^{+} + HY^{-} \xrightarrow{k_{VI}} [Cr(OH)(HY)_2(H_2O)_2] \quad (60)$$

$$[Cr(OH)(HY)_2(H_2O)_2] \longrightarrow [Cr(Y)(HY)(H_2O)_2] + H_2O \quad (61)$$

Assuming now that the penta-coordinated intermediate formed in the new slow step is reactive enough to be in steady state, and applying again to eq 58 the quasi-equilibrium approximation, the expression obtained for the second experimental rate constant is as follows:

$$k_2 = \frac{K_{IV}\ k_V\ k_{VI}\ [HY^-]}{(k_{-V} + k_{VI}\ [HY^-])\ [H^+]} \quad (62)$$

Equation 62 is consistent with the kinetic data corresponding to the dependences of k_2 on the initial concentrations of organic ligand (Figure 12, right, bottom) and hydrogen ion (Figure 14, bottom). Moreover, the increasing effect of the ionic strength (Figure 13, bottom), albeit difficult to explain, might be the result of a combined complex dependence of equilibrium constant K_{IV} and rate constants k_V, k_{-V} and k_{VI}. The difference with rate constant k_1 (decreasing with the ionic strength) may be the consequence of the loss in electrostatic charge of the three cations

involved as reactants in eqs 58-60 with respect to those involved in eqs 53-55 caused by the coordination of the anionic ligand HY^- to Cr(III).

Of all the rate constants appearing in eqs 57 and 62, the ones suspected to have a biggest incidence in the magnitude of the experimental activation energies are k_{II} (in relation to k_1) and k_V (in relation to k_2). Hence, the notably high values of these parameters ($E_{a,1}$ = 83 kJmol^{-1} and $E_{a,2}$ = 95 kJmol^{-1}) suggest that the loss of an aqua ligand from the first coordination sphere of the metal ion (as in eqs 54 and 59) involves a rather large energy requirement because of the chemical inertness of Cr(III) complexes.

Given enough time (at $t = \infty$), the following equilibria might be reached:

$$[Cr(Y)(HY)(H_2O)_2] + HY^- \rightleftarrows [Cr(Y)(HY)_2]^- + 2\,H_2O \quad (63)$$

$$[Cr(Y)(HY)_2]^- \rightleftarrows [Cr(Y)_2(HY)]^{2-} + H^+ \quad (64)$$

where the complexes $[Cr(Y)(HY)(H_2O)_2]$, $[Cr(Y)(HY)_2]^-$ and $[Cr(Y)_2(HY)]^{2-}$ correspond to C_n , $C_{n+1} - H^+$ and C_{n+1} (see eqs 1 and 11), respectively. Coordination to the cationic metal ion is expected to result in a decrease of the electron density of the labile hydrogen atoms of the organic ligand, and so in a parallel increase of the corresponding acidity equilibrium constant. Since, to explain the data shown in Figure 6 (bottom, left and right), the pK_a associated to eq 64 should be close to the experimental pH range (5.01 – 5.87) and, given the three pK_a values reported for L-glutamic acid,[49] the most probable functional group whose deprotonation is implicated in eq 64 might be the amino substituent.

12. SOME ADDITIONAL DATA

The number of hydrogen ions released to the medium during the course of the reaction (per chromium atom belonging to the violet complex) has been estimated from the experimental values of the final pH at different initial concentrations of metal ion and sodium hydrogen L-glutamate (Table 9), considering for that purpose two of the amino acid dissociation equilibria:

$$HO_2C(CH_2)_2CH(NH_3^+)CO_2^- \rightleftarrows {}^-O_2C(CH_2)_2CH(NH_3^+)CO_2^- + H^+ \quad (65)$$

$${}^-O_2C(CH_2)_2CH(NH_3^+)CO_2^- \rightleftarrows {}^-O_2C(CH_2)_2CH(NH_2)CO_2^- + H^+ \quad (66)$$

the corresponding pK_a data (4.07 and 9.47 at 25.0 ºC) being the ones relevant to the experimental pH range (4.53 – 5.87).[49]

$[Cr(NO_3)_3]_o$ $[10^{-2}$ M]	$[Ligand]_o$ [M]	Number (H^+)
0.59	0.392	1.32 ± 0.02
1.18	0.392	1.24 ± 0.02
1.76	0.392	1.22 ± 0.01
2.35	0.392	1.24 ± 0.01
2.94	0.392	1.22 ± 0.01
3.53	0.392	1.22 ± 0.02
4.12	0.392	1.21 ± 0.02
4.71	0.392	1.24 ± 0.01
5.29	0.392	1.26 ± 0.01
5.88	0.392	1.27 ± 0.01
6.47	0.392	1.31 ± 0.01
0.59	0.049	1.21 ± 0.01
0.59	0.098	1.24 ± 0.01
0.59	0.147	1.29 ± 0.01
0.59	0.196	1.30 ± 0.01
0.59	0.245	1.32 ± 0.02
0.59	0.294	1.30 ± 0.01
0.59	0.343	1.32 ± 0.02
0.59	0.441	1.31 ± 0.02
0.59	0.490	1.28 ± 0.01

(a) The final pH values were in the range 4.53 — 5.87.

Table 9. Number of hydrogen ions released to the medium per chromium atom in the violet complex at different initial concentrations of metal ion and organic ligand (sodium hydrogen L-glutamate) and 25.0 ºC.

It can be observed that the number of hydrogen ions released is rather independent of the reactant initial concentrations, the average value being 1.27 ± 0.04. This result is coherent with

the proposed mechanism since, according to it, one hydrogen ion is released in an irreversible way:

$$[Cr(H_2O)_6]^{3+} + 2\ HY^- \longrightarrow [Cr(Y)(HY)(H_2O)_2] + H^+ + 4\ H_2O \qquad (67)$$

equation 67 having been obtained by addition of eqs 53-56 and 58-61. Moreover, a second hydrogen ion is released in a reversible way (eq 64), yielding a global value intermediary between 1 and 2.

On the other hand, it might be interesting to have some information on the behavior of the long-lived intermediate toward the UV-Vis radiation. Since the spectrum of the intermediate could not be directly recorded, given that at any moment during the course of the reaction it is always present in a mixture with the reactant and the product (the three of them absorbing light), some rather complex calculations were required for that purpose. They started with the localization of the instant at which the long-lived intermediate reaches its maximum concentration. By derivation in eq 42 and equaling the result to zero, it can be inferred that:

$$t_{max} = \frac{1}{k_1 - k_2} \ln \frac{k_1}{k_2} \qquad (68)$$

$$[I]_{max} = \frac{k_1}{k_2} [R]_o\ e^{-k_1 t_{max}} \qquad (69)$$

Application of eqs 68 and 69 to the kinetic experiment corresponding to Figure 2, for which a periodic scanning of the UV-Vis spectra during the course of the reaction was recorded, allowed the estimation of both t_{max} and $[I]_{max}$ for this particular case. Interpolation between the two intermediary spectra closer to that instant led to the spectrum of the reacting mixture at the exact moment when the long-lived intermediate exhibited its maximum concentration. Then, the molar absorption coefficient of the intermediate at each wavelength could be obtained by discounting from the total absorbance (A_λ) the contributions of the other two chemical species absorbing light:

$$\varepsilon_{I,\lambda} = \frac{A_\lambda - (\varepsilon_{R,\lambda} [R]_{max} + \varepsilon_{P,\lambda} [P]_{max})\, l}{[I]_{max}\, l} \qquad (70)$$

$[R]_{max}$ (obtained from eq 39) and $[P]_{max}$ (obtained from eq 43) being the concentrations of reactant and product, respectively, at the instant t_{max}, whereas the other symbols have the same meaning than in eq 44. The results obtained from eq 70 have been plotted in order to be compared with the spectral data experimentally accessible for the inorganic reactant and the final product (Figure 17).

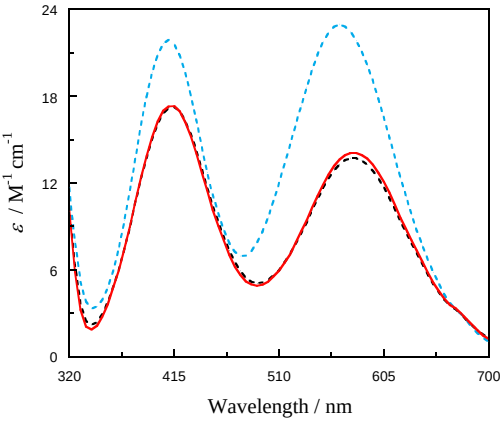

Figure 17. Molar absorption coefficients as a function of the wavelength for the UV-Vis spectra of three Cr(III) complexes: reactant (black dashed line), long-lived intermediate (red continuous line) and final product (blue dashed line). $[Cr(NO_3)_3]_o = 2.65 \times 10^{-2}$ M, [L-glutamic acid]$_o$ = 3.92×10^{-2} M, $[KOH]_o = 1.62 \times 10^{-2}$ M, pH 2.59, 25.0 ºC.

It can be concluded that the spectrum of the long-lived intermediate is quite similar to that of the inorganic reactant, but with the two maximum peaks slightly more intense, what is indeed consistent with the value of parameter *Q* a little higher than 1 taken previously in eq 47 to fit the experimental absorbance-time data.

The same procedure was repeated using this time sodium hydrogen L-glutamate instead of L-glutamic acid as the source of organic ligands. Given that, due to the higher pH, the reaction was now considerably faster than that performed under the experimental conditions corresponding to Figure 2, the periodic scanning could be done until a higher extent of reaction. The main difference with the former situation is that now three isosbestic points can be observed (Figure 18, left). Although the existence of a perfect isosbestic point would require that the total absorbance of the solution at a particular wavelength remain constant during the course of the reaction, the second point is not well defined because of the participation of a

long-lived intermediate in the mechanism. Once again, the electronic spectrum calculated for this species when the organic reactant was sodium hydrogen L-glutamate was also much more similar to that of the inorganic reactant than to that of the product (Figure 18, right). This might bear some importance regarding the structure of the intermediate.

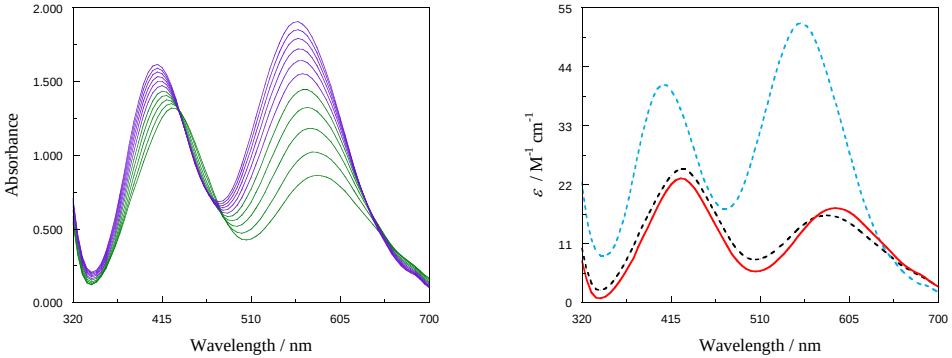

Figure 18. Left: periodic scanning of the UV-Vis spectrum at 3-min time intervals. The shift from green to violet indicates the progress of the reaction. Right: molar absorption coefficients as a function of the wavelength for three Cr(III) complexes: reactant (black dashed line), long-lived intermediate (red continuous line) and final product (blue dashed line). $[Cr(NO_3)_3]_o$ = 5.29 × 10^{-2} M, [sodium hydrogen L-glutamate]$_o$ = 0.392 M, pH 4.68, 25.0 ºC.

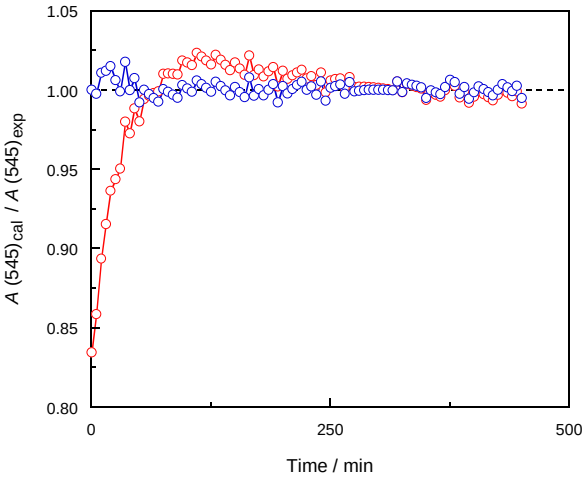

Figure 19. Ratio between the calculated and experimental absorbances at 545 nm as a function of time during the course of the reaction. Red: one rate constant (pseudo-first order) kinetic model. Blue: two rate constant (double-exponential) kinetic model. $[Cr(NO_3)_3]_o$ = 5.88 × 10^{-3} M, [L-glutamic acid]$_o$ = 3.43 × 10^{-2} M, $[KOH]_o$ = 2.03 × 10^{-2} M, pH 3.45, 25.0 ºC.

Furthermore, given that the Cr(III)/L-glutamic acid reaction (under conditions of a large excess of organic ligand) has been previously reported in the chemical literature to follow a pseudo-first order behavior, it might be worth to compare the quality of the absorbance-time fits attained with two mathematical alternatives: the oversimplified one rate constant kinetic model and the two rate constant kinetic model used in the present work. As can be seen in Figure 19, the ratio between the calculated and experimental absorbances during the course of the reaction was much closer to unity when two rate constants were employed in the fit. The failure of the pseudo-first order model was especially notable in the first part of the reaction, since the calculated absorbances were systematically lower than their experimental counterparts.

Finally, it should be mentioned that the two rate constant kinetic model presents indeed some limitations. Among them, we can enumerate the following:

(i) The pH of the reacting mixtures decreased during the experiments due to the release of hydrogen ions from the organic substrate to the medium as the complexation advanced.

(ii) Given the chemical inertness to substitution of Cr(III) complexes, it is likely that the metal ion-aqua bonds belonging to the initial inorganic reactant be broken in several consecutive slow steps, resulting in the appearance of more than one long-lived intermediate.

However, all in all and considering the complexity of the chemical problem under study, the kinetic model used to obtain the reaction parameters should be considered as a good enough approximation to the real behavior of nature.

13. CHROMIUM (III) / L-GLUTAMATE COMPLEX STRUCTURE

The organic ions involved in the complexes formed as a long-lived intermediate in eq 56 and as reaction products in eqs 61, 63 and 64 behave as bidentate ligands, each containing an oxygen atom belonging to a carboxylate group and a nitrogen atom belonging to an amino group as electron-pair donors to the metal ion. The carboxylate group coordinated to Cr(III) is, in all likelihood, the one occupying the C5 position of the amino acid chain, since the oxygen

atoms belonging to that in the C1 position are expected to possess a lower electron density because of the withdrawing inductive effect caused by the vicinal amino group. A tentative structure proposed for the complexes with the highest number of organic ligands, $[Cr(Y)(HY)_2]^-$ and $[Cr(Y)_2(HY)]^{2-}$, is shown in Figure 20. Actually, a Cr(III)-glutamic acid complex including three organic ligands has been reported.[23] Similar structures have been proposed for EDTA[50-52] and EDTA-type[53] complexes of Cr(III) and other transition metal ions.

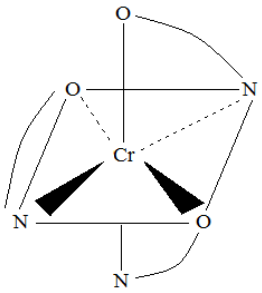

Figure 20. Schematic drawing of the proposed structure for the final violet complex involving three organic ions (hydrogen L-glutamate or L-glutamate) as ligands, with both oxygen atoms from the C5 carboxylate groups and nitrogen atoms from the amino groups as electron-pair donors to the metal ion placed in the center of the octahedron.

The participation of the nitrogen atoms as electron-pair donors (Lewis bases) to the transition metal center (Lewis acid), in addition to that of carboxylate-belonging oxygen atoms, is supported by the finding of L-glutamic acid precipitation after completion of the kinetic monitoring of the reaction in the experiments performed at high initial concentrations of Cr(III) ($\geq 4.71 \times 10^{-2}$ M) and sodium hydrogen L-glutamate (0.392 M). This circumstance can be related to the low water solubility of L-glutamic acid in contrast with that of its monosodium salt. Since the only acidic hydrogen atoms in aqueous hydrogen L-glutamate ion are those belonging to the protonated amino group, it can be inferred that deprotonation of the latter is a requirement for the final violet complex to be formed, so that the consequent liberation of hydrogen ions is the cause of the observed precipitation.

14. CONCLUSIONS

(i) Chromium (III) forms a highly stable complex with L-glutamic acid / hydrogen L-glutamate ion in aqueous media, the color of the solution changing from blue (at low pH) or green (at high pH) to violet. The formation of the final complex can be monitored spectrophotometrically at a wavelength of 530 – 555 nm, range for which the increase of absorbance during the kinetic runs presents a maximum.

(ii) The UV-Vis spectroscopy data strongly suggest the coexistence of several complexes (differing in the number of organic ligands as well as in their acid-base properties) in the final reacting mixture.

(iii) The kinetics of the reaction, even in the presence of a large excess of ligand, does not follow a pseudo-first-order behavior (as previously proposed in the chemistry literature). Actually, the rate-time plots showed a clear-cut bell-shaped profile, with an acceleration period followed by a deceleration one.

(iv) The unusual pattern of the rate-time plots cannot be attributed to an autocatalytic phenomenon. Instead, the acceleration period can be explained by the accumulation of a long-lived intermediate in the solution, not being reactive enough for the steady state approximation to apply.

(v) A BASIC-language program, using a double-exponential integrated rate law and designed to change systematically the fitting parameters, has allowed the determination of two experimental rate constants for each kinetic run, corresponding to the formation of the long-lived intermediate from the reactants (k_1) and to its decay into the final violet product (k_2).

(vi) When sodium hydrogen L-glutamate was used as organic substrate, both rate constants increased with the ligand initial concentration, following a double-reciprocal law.

(vii) Addition of potassium nitrate as background electrolyte resulted in a decrease of rate constant k_1 and in an increase of k_2. Moreover, both experimental rate constants increased with increasing pH, indicating the existence of a phenomenon of base catalysis.

(viii) Rate constant k_1 was one order of magnitude higher than k_2, and the respective activation energies were 83 ± 10 and 95 ± 5 kJ mol^{-1}, indicating that the formation of the long-lived intermediate was much faster than its decay.

(ix) A reaction mechanism, involving a long-lived intermediate and consistent with the experimental information available on rate constants k_1 and k_2, has been proposed. The key (slow) steps of this mechanism imply the breakage of Cr(III)-H_2O chemical bonds, thus leaving a vacant coordination place to allow the entrance of the organic ligand.

(x) The singular kinetic behavior of this reaction is a consequence of the combined effects of the inertness to substitution of the Cr(III)-ligand chemical bonds and the polydentate character of L-glutamic acid / hydrogen L-glutamate ion as complexing agents.

15. REFERENCES

1. Perez Benito, J. F.; Arias, C.; Rodriguez, R. M. Reactivities of D-Mannitol and Related Alcohols toward Chromium(VI) and Chromium(IV). *J. Phys. Chem. A* **2001**, *105,* 1150-1157.
2. Ghosh, S. P.; Kumar, M.; Koley, A. P.; Ghosh, M. C. First Direct Detection of Chromium(IV) as a Long Lived Intermediate in the Oxidation of Methanol by Chromium(VI). *J. Chem. Res. S* **2003**, *6,* 346-347.
3. Bertoni, F. A.; Bellu, S. E.; Gonzalez, J. C.; Sala, L. F. Reduction of Hypervalent Chromium in Acidic Media by Alginic Acid. *Carbohydr. Polym.* **2014**, *114,* 1-11.
4. Mertz, W. Chromium and its Relation to Carbohydrate Metabolism. *Med. Clin. N. Am.* **1976**, *60,* 739-744.
5. Mertz, W. Chromium in Human Nutrition. A Review. *J. Nutr.* **1993**, *123*, 626-633.
6. Schwarz, K.; Mertz, W. Chromium(III) and the Glucose Tolerance Factor. *Arch. Biochem. Biophys.* **1959**, *85*, 292-295.
7. Weksler-Zangen, S.; Mizrahi, T.; Raz, I.; Mirsky, N. Glucose Tolerance Factor Extracted from Yeast: Oral Insulin-Mimetic and Insulin-Potentiating Agent: In Vivo and In Vitro Studies. *Br. J. Nutr.* **2012**, *108*, 875-882.
8. Liu, L.; Cui, W. M.; Zhang, S. W.; Kong, F. H.; Pedersen, M. A.; Wen, Y.; Lv, J. P. Effect of Glucose Tolerance Factor (GTF) from High Chromium Yeast on Glucose Metabolism in Insulin-Resistant 3T3-L1 Adipocytes. *RSC Adv.* **2015**, *5,* 3482-3490.
9. Cefalu, W. T.; Hu, F. B. Role of Chromium in Human Health and in Diabetes. *Diabetes Care* **2004**, *27,* 2741-2751.
10. Mirsky, N.; Cohen, R.; Eliaz, A.; Dovrat, A. Inhibition of Diabetic Cataract by Glucose Tolerance Factor Extracted from Yeast. *Exp. Biol. Med.* **2016**, *241,* 817-829.
11. Chen, Y.; Watson, H. M.; Gao, J. J.; Sinha, S. H.; Cassady, C. J.; Vincent, J. B. Characterization of the Organic Component of Low Molecular Weight Chromium Binding Substance and its Binding of Chromium. *J. Nutr.* **2011**, *141,* 1225-1232.
12. McCarty, M. F. Longevity Effect of Chromium Picolinate Rejuvenation of Hypothalamic Function. *Med. Hypotheses* **1994**, *43*, 253-265.
13. Sivakumar, S.; Subbhuraam, C. V. Toxicity of Chromium(III) and Chromium(VI) to the Earthworm *Eisenia fetida*. *Ecotoxicol. Environm. Safety* **2005**, *62*, 93-98.
14. Takahashi, T.; Toda, E.; Singh, R. B.; De Meester, F.; Wilczynska, A.; Wilson, D.; Juneka, L. R. Essential and Non-Essential Amino Acids in Relation to Glutamate. *Open Nutraceut. J.* **2011**, *4,* 205-212.
15. Perez Benito, J. F.; Lamrhari, D.; Arias, C. Three Rate Constants from a Single Kinetic Experiment: Formation, Decomposition and Reactivity of the Chromium(VI) Glutathione Thioester Intermediate. *J. Phys. Chem.* **1994**, *98,* 12621-12629.
16. Jacob, R. A. The Integrated Antioxidant System. *Nutr. Res.* **1995**, *15,* 755-766.
17. Arthur, J. R. The Glutathione Peroxidases. *Cell. Mol. Life Sci.* **2000**, *57,* 1825-1835.
18. Mahieu, S.; Klug, M.; Millen, N.; Fabro, A.; Benmelej, A.; Contini, M. C. Monosodium Glutamate Intake Affects the Function of the Kidney Through NMDA Receptor. *Life Sciences* **2016,** *149,* 114-119.
19. Bakac, A.; Espenson, J. H. Chromium Complexes Derived from Molecular Oxygen. *Acc. Chem. Res.* **1993,** *26,* 519-523.
20. Kornev, V. I.; Mikryukova, G. A. Coordination Compounds of Chromium(III) with Different Complexones and Citric Acid in Aqueous Solutions. *Russ. J. Coord. Chem.* **2004**, *30*, 895-899.
21. Perez-Benito, J. F. Effects of Chromium(VI) and Vanadium(V) on the Lifespan of Fish. *J. Trace Elem. Med. Biol.* **2006,** *20,* 161-170.
22. Guindy, N. M.; Abou-Gamra, Z. M.; Abdel-Messih, M. F. Kinetic Studies on the Complexation of Aqua Chromium(III) with DL-Leucine in Aqueous Acidic Media. *J. Chim. Phys.* **1999,** *96,* 851-864.

23. Guindy, N. M.; Abou-Gamra, Z. M.; Abdel-Messih, M. F. Kinetic Studies on the Complexation of Chromium(III) with some Amino Acids in Aqueous Acidic Medium. *Monatsh. Chem.* **2000,** *131,* 857-866.
24. Abdel Messih, M. F.; Abou-Gamra, Z. M. Kinetic and Mechanism of the Reaction between Chromium(III) and Picolinic Acid in Weak Acidic Aqueous Solution. *Monatsh. Chem.* **2012,** *143,* 211-216.
25. Hamm, R. E. Complex Ions of Chromium. IV. The Ethylenediaminetetraacetic Acid Complex with Chromium(III). *J. Am. Chem. Soc*. **1953**, *75*, 5670-5672.
26. Hedrick, C. E. Formation of the Chromium-EDTA Complex. *J. Chem. Educ.* **1965**, *42*, 479-480.
27. Barreto, J. C.; Brown, D.; Dubetz, T.; Kakareka, J.; Alberte, R. S. A Spectrophotometric Determination of the Energy of Activation (E_a) for a Complexation Reaction: The Kinetics of Formation of a Cr(III)/EDTA Complex. *Chem. Educator* **2005**, *10*, 196-199.
28. Perez-Benito, J. F. Two Rate Constant Kinetic Model for the Chromium(III)-EDTA Complexation Reaction by Numerical Simulations. *Int. J. Chem. Kinet.* **2017,** *49,* 234-249.
29. Abdel-Messih, M. F. Kinetics and Mechanism of Interaction between Chromium(III) and Ethylenediaminetetrapropinoate in Aqueous Acidic Media. *Adv. Chem. Eng. Sci.* **2013,** *3,* 98-104.
30. Volk, L.; Richardson, W.; Lau, K. H.; Hall, M.; Lin, S. H. Steady State and Equilibrium Approximations in Reaction Kinetics. *J. Chem. Educ.* **1977**, *54*, 95-97.
31. Wilkinson, F. *Chemical Kinetics and Reaction Mechanisms*; Van Nostrand Reinhold: New York, 1980.
32. Roque, C.; Pimienta, V.; Lavabre, D.; Micheau, J. C. Occurrence of Multiple Steady States in the Biphasic Alkaline Hydrolysis of C-4 to C-8 Ethyl Alkanoates. *J. Phys. Chem. A* **2001**, *105,* 5877-5880.
33. Perez-Benito, J. F.; Ferrando, J. Three Rate-Constant Kinetic Model for Permanganate Reactions Autocatalyzed by Colloidal Manganese Dioxide: the Oxidation of L-Phenylalanine. *J. Phys. Chem. B* **2014**, *118,* 14949-14960.
34. Hu, Y.; Horvath, A. K.; Duan, S. S.; Cseko, G.; Makarov, S. V.; Gao, Q. Y. Mechanism Involving Hydrogen Sulfite Ions, Chlorite Ions, and Hypochlorous Acid as Key Intermediates of the Autocatalytic Chlorine Dioxide-Thiourea Dioxide Reaction. *Eur. J. Inorg. Chem.* **2015**, 5011-5020.
35. Espenson, J. H. *Chemical Kinetics and Reaction Mechanisms*; McGraw-Hill: New York, 1995.
36. Laidler, K. J. *Chemical Kinetics*; Harper Collins: New York, 1987.
37. Atkins, P. W.; de Paula, J. *Physical Chemistry*; University Press: Oxford, 2006.
38. Berberan-Santos, M. N.; Martinho, J. M. G. The Integration of Kinetic Rate Equations by Matrix Methods. *J. Chem. Educ.* **1990**, 67, 375-379.
39. Levine, I. N. *Physical Chemistry*; McGraw-Hill: New York, 2002.
40. Perez-Benito, J. F.; Arias, C. A Kinetic Study of the Permanganate Oxidation of Triethylamine. Catalysis by Soluble Colloids. *Int. J. Chem. Kinet.* **1991**, *23,* 717-732.
41. Perez-Benito, J. F.; Arias, C.; Amat, E. A Kinetic Study of the Reduction of Colloidal Manganese Dioxide by Oxalic Acid. *J. Colloid Interface Sci.* **1996**, *177*, 288-297.
42. Perez-Benito, J. F.; Arias, C. A Kinetic Study of the Oxidation of L-Ascorbic Acid by Chromium(VI). *Int. J. Chem. Kinet*. **1993**, *25*, 221-227.
43. Mata-Perez, F.; Perez-Benito, J. F. Kinetics and Mechanisms of Oxidation of Methylamine by Permanganate Ion. *Can. J. Chem.* **1987**, *65*, 2373-2379.
44. L'vov, B. V.; Galwey, A. K. Interpretation of the Kinetic Compensation Effect in Heterogeneous Reactions: Thermochemical Approach. *Int. Rev. Phys. Chem.* **2013**, *32*, 515-557.
45. Robinson, P. J. Dimensions and Standard States in the Activated Complex Theory of Reaction Rates. *J. Chem. Educ.* **1978**, 55, 509-510.
46. Perez Benito, J. F. Some Tentative Explanations for the Enthalpy-Entropy Compensation Effect in Chemical Kinetics: from Experimental Errors to the Hinshelwood-Like Model. *Monatsh. Chem.* **2013**, *144,* 49-58.

47. Stünzi, H.; Marty, W. Early Stages of the Hydrolysis of Chromium(III) in Aqueous Solution. 1. Characterization of a Tetrameric Species. *Inorg. Chem.* **1983**, *22*, 2145-2150.
48. Galstyan, G.; Knapp, E. W. Computing pK_a Values of Hexa-Aqua Transition Metal Complexes. *J. Comput. Chem.* **2015**, *36*, 69-78.
49. Coetzee, J. F.; Ritchie, C. D. *Solute-Solvent Interactions*; Dekker: New York, 1969.
50. Gerdom, L. E.; Baenziger, N. A.; Goff, H. M. Crystal and Molecular Structure of a Substitution-Labile Chromium(III) Complex: Aquo(ethylenediaminetriacetatoacetic Acid)Chromium(III). *Inorg. Chem.* **1981**, *20*, 1606-1609.
51. Wheeler W. D.; Legg, J. I. Solution Structure of the Cr(III) Complex with EDTA by Deuteron NMR Spectroscopy. *Inorg. Chem.* **1984**, *23*, 3798-3802.
52. Kanamori, K.; Kawai, K. Raman Spectral Study on the Solution Structure of the Chromium(III)-EDTA Complex. *Inorg. Chem.* **1986**, *25*, 3711-3713.
53. Grubisic, S.; Radanovic, D. D.; Rychlewska, U.; Warzajtis, B.; Draskovic, N. S.; Djuran, M. I.; Niketic, S. R. Conformational Study of Co(II), Ni(II), and Cr(III) Complexes of the EDTA--Type: Crystal Structure of 1D Polymeric Trans(O^6)-Ba[Co(1,3-pddadp)]·8H_2O Complex Stabilized by Infinite Water Tapes. *Polyhedron* **2007**, *26*, 3437-3447.